Breaking waves are generally divided into three main types, depending on the steepness of the waves and the slope of the shoreface:

Spilling takes place when steep waves propagate over **flat shorefaces.** Spilling breaking is a gradual breaking which takes place as a foam bore on the front topside of the wave over a distance of 6-7 wavelengths.

Plunging is the form of breaking where the upper part of the wave breaks over its own lower part in one **big splash** whereby most of the energy is lost. This form of breaking takes place in case of **moderately steep waves on a moderately sloping shoreface.**

Surging is when the lower part of the wave surges up on the foreshore in which case there is hardly any surf-zone. This form of breaking takes place when relatively long waves (swell) meet **steep shorefaces**.

Depth-induced wave-breaking: spilling, plunging and surging

White-capping or top-breaking is steepness-induced wave-breaking which occurs on deeper water when the wave height becomes **too large compared to the wavelength**.

Wave-overtopping takes place when waves meet a submerged reef or structure, but also when waves meet an emerged reef or structure lower than the approximate wave height. During over-topping, two processes of importance for the coastal processes take place: **wave transmission and passing of water over the structure.**

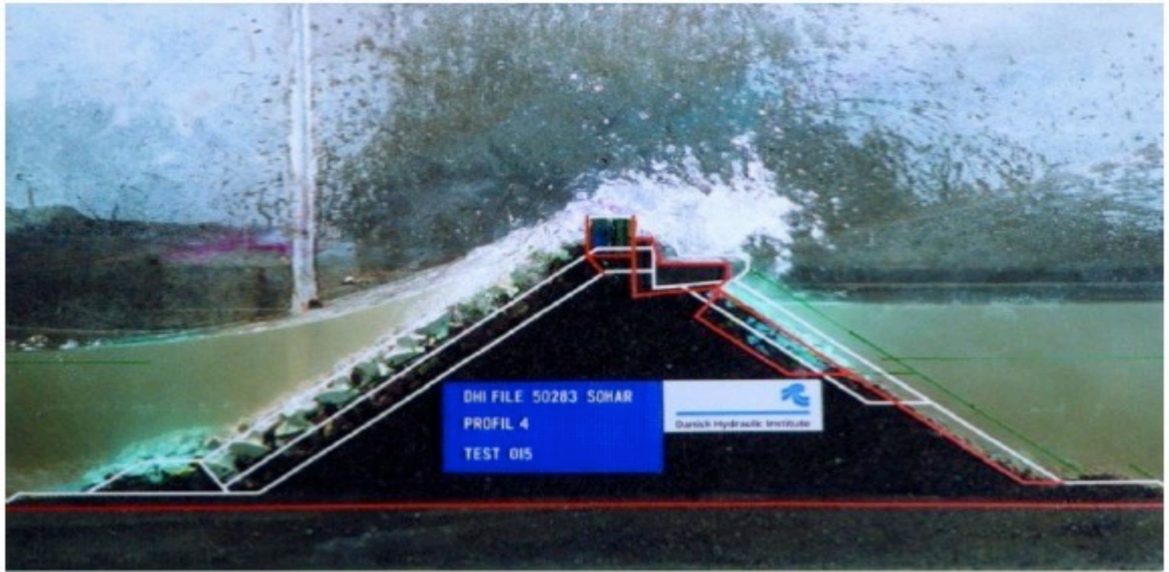
DHI FILE 50283 SOHAR
PROFIL 4
TEST 015
Danish Hydraulic Institute

LONGSHORE SEDIMENT TRANSPORT

The breaking waves and surf in the nearshore combine with various horizontal and vertical patterns of nearshore currents to transport beach sediments. Sometimes this transport results only in a local rearrangement of sand into *bars* and *troughs*, or into a *series of rhythmic embayments* cut into the beach. At other times there are extensive longshore displacements of sediments, possibly moving hundreds of thousands of cubic meters of sand *along the coast each year*.

We introduce the techniques that have been developed to evaluate the longshore sediment transport rate, which is defined to occur primarily within the surf zone, directed parallel to the coast.

This transport is among the most important nearshore processes that control the *beach morphology*, and determines in large part whether shores erode, accrete, or remain stable.

Currents associated with nearshore cell circulation generally act to produce *only a local rearrangement of beach sediments*.

The rip currents of the circulation can be important in the **cross-shore** transport of sand, but there is minimal net of beach sediments along the coast. More important to the longshore movement of sediments are *waves breaking obliquely* to the coast and the *longshore currents* they generate, which may flow along *an extended length of beach*.

The resulting movement of beach sediment along the coast is referred to as *littoral transport or longshore sediment transport*, whereas the actual volumes of sand involved in the transport are termed the littoral drift.

This longshore movement of beach sediments is of particular importance in that the transport can either be interrupted by the construction of jetties and breakwaters, or can be captured by inlets and submarine canyons.

Littoral transport can also result from the currents generated by alongshore gradients in breaking wave height, commonly called *diffraction currents*.

This transport is manifest as a movement of beach sediments toward the structures which create these diffraction currents (such as jetties, long groins, and headlands). The result is transport in the "upwave" direction on the downdrift side of the structure.

This, in turn, can create a buildup of sediment on the immediate, downdrift side of the structure or contribute to the creation of a crenulate-shaped shoreline on the downdrift side of a headland.

On most coasts, waves reach the beach from different quadrants, producing day-to-day and seasonal reversals in transport direction. At a particular beach site, transport may be to the right (lookin seaward) during part of the year and to the left during the remainder of the year. If the left and right transports are denoted respectively Q_L and Q_R, with Q_R being assigned a positive quantity and Q_L assigned a negative value for transport direction clarification purposes, then the net annual transport is defined as

$$Q_{NET} = Q_L + Q_R.$$

The net longshore sediment transport rate is therefore directed right and positive if $Q_R > Q_L$, and to the left and negative if $Q_R < Q_L$.

The net annual transport can range from essentially zero to a large magnitude, estimated at a million cubic meters of sand per year for some coastal sites. The gross annual longshore transport is defined as

$$Q_{GROSS} = abs(Q_R) + abs(Q_L),$$

the sum of the temporal magnitudes of littoral transport irrespective of direction. It is possible to have a very large gross longshore transport at a beach site while the net transport is effectively zero.

These two contrasting assessments of longshore sediment movements have **different engineering applications**.

A distinction is made between two *modes of sediment transport*: suspended sediment transport, in which sediment is carried **above the bottom** by the turbulent eddies of the water, and **bed-load sediment** transport, in which the grains remain close to the bed and move by rolling and jumping.

Because it is more readily measured than the bed-load transport, suspended load transport has been the subject of considerable study. It has been demonstrated that suspension concentrations decrease with height above the bottom. The highest concentrations typically are found in the breaker and swash zones, with lower concentrations at midsurf positions.

On *reflective beaches*, at which a portion of the wave energy is reflected back to sea, individual suspension events are correlated with the incident breaking wave period.

In contrast, on *dissipative beaches*, at which effectively all of the arriving wave energy is dissipated in the nearshore, long-period infragravity water motions have been found to account for significant sediment suspension.


Venezia
Trieste
Genova
Ancona
Roma
Bari
Napoli
Cagliari
Catanzaro
Palermo
Costa alta
Spiaggia
Spiaggia stabile
Spiaggia in arretramento
Spiaggia in avanzamento

In engineering applications, the longshore sediment transport rate is expressed as the volume transport rate Q_l having units such as cubic meters per day or per year.
This is the total volume as would be measured by survey of an impoundment at a jetty and includes about 40 percent void space between the particles as well as the 60-percent solid grains.

Another representation of the longshore sediment transport rate is an immersed weight transport rate I_ℓ related to the volume transport rate by

$$I_\ell = (\rho_s - \rho)\, g\, (1 - n)\, Q_\ell$$

The potential longshore sediment P_ℓ transport rate, dependent on an available quantity of littoral material, is most commonly correlated with the so-called longshore component of wave energy flux or power.

$$P_\ell = (EC_g)_b \sin\alpha_b \cos\alpha_b$$

It is necessary to know E_b - the wave energy evaluated at the breaker line and the the C_{gb} wave group speed at the breaker line . The immersed weight transport rate I_ℓ has the same units as P (N/s), so that the relationship

$$I_\ell = KP_\ell$$

is homogeneous, that is, the empirical proportionality coefficient K is dimensionless

Field data relating I and P are plotted in the following figure, for which the calculations of the wave power are based on the root-mean-square wave height at breaking H . Data presented in the figure include field data measured from different author

The K coefficient defined here is based on utilizing the rms breaking wave height H. The Shore Protection Manual (1984) presented a dimensionless coefficient K = (0.39) based on computations utilizing the significant wave height.

The value of this coefficient corresponding to the rms wave height H is **K = 0.92**, which is indicated in the next figure with a dashed line for reference.. The dash-double-dot lines represent a ±50 percent interval around the SPM reference line (K = 0.92).

An early design value of the K coefficient was introduced for use with rms breaking wave height by Komar and Inman (1970); **K = 0.77**. This value is commonly seen in many longshore transport rate and computations.

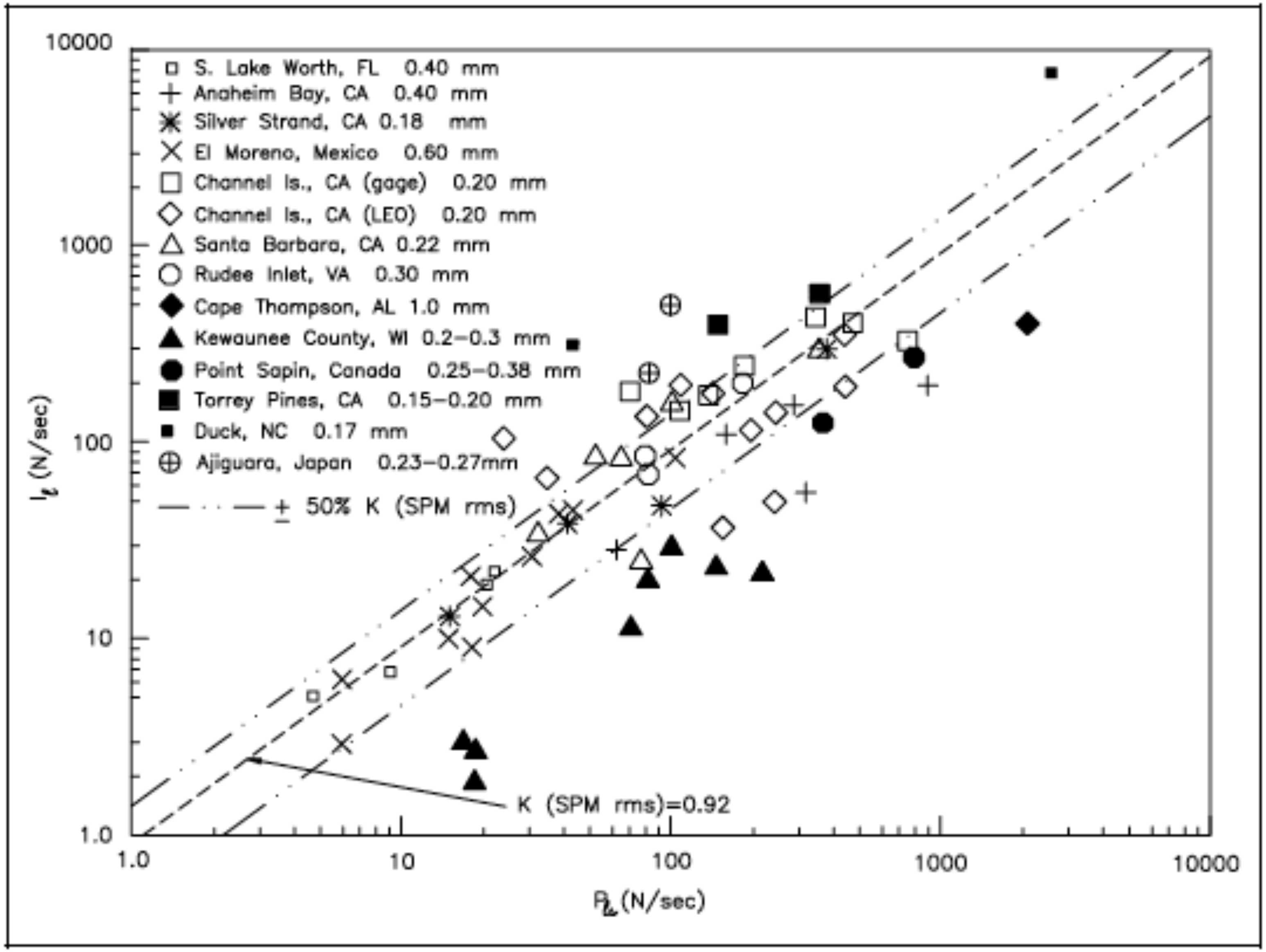

10000
1000
100
10
1.0
S. Lake Worth, FL 0.40 mm
Anaheim Bay, CA 0.40 mm
Silver Strand, CA 0.18 mm
El Moreno, Mexico 0.60 mm
Channel Is., CA (gage) 0.20 mm
Channel Is., CA (LEO) 0.20 mm
Santa Barbara, CA 0.22 mm
Rudee Inlet, VA 0.30 mm
Cape Thompson, AL 1.0 mm
Kewaunee County, WI 0.2–0.3 mm
Point Sapin, Canada 0.25–0.38 mm
Torrey Pines, CA 0.15–0.20 mm
Duck, NC 0.17 mm
Ajiguara, Japan 0.23–0.27mm
± 50% K (SPM rms)
K (SPM rms)=0.92
I_ℓ (N/sec)
1.0
10
100
1000
10000
$P_{\ell s}$ (N/sec)

Some works have domostrated that the sand transport in the nearshore results from the combined effects of waves and currents; i.e., the waves placing sand in motion and the longshore currents producing a net sand advection. Walton (1980, 1982) proposed a longshore sediment transport calculation method using the breaking-wave-driven longshore current model of Longuet-Higgins (1970) from which the longshore energy flux factor becomes

$$P_\ell = \frac{\rho\, g\, H_b\, W\, V_\ell\, C_f}{\left(\frac{5\pi}{2}\right)\left(\frac{V}{V_o}\right)}$$

in which W is the width of the surf zone, V_l is the measured longshore current at a point in the surf zone, C_f is a friction coefficient dependent on Reynolds' number and bottom roughness, and V_o is the theoretical longshore velocity at breaking for the no-lateral-mixing case.

Longshore sediment transport is a fluctuating quantity which can be depicted as shown in the next figure, where positive sediment transport is defined as **positive** in value if toward the right for an observer looking seaward from the beach, and **negative** in value if sediment transport is toward the left as noted previously.

In terms of "Q_ℓ ," the net longshore sediment transport rate is the "time average" transport given by

$$\overline{Q_\ell} = \frac{1}{T_o} \int_o^{T_o} Q_\ell(t)\, dt$$

LONGSHORE WAVE INDUCED TRANSPORT

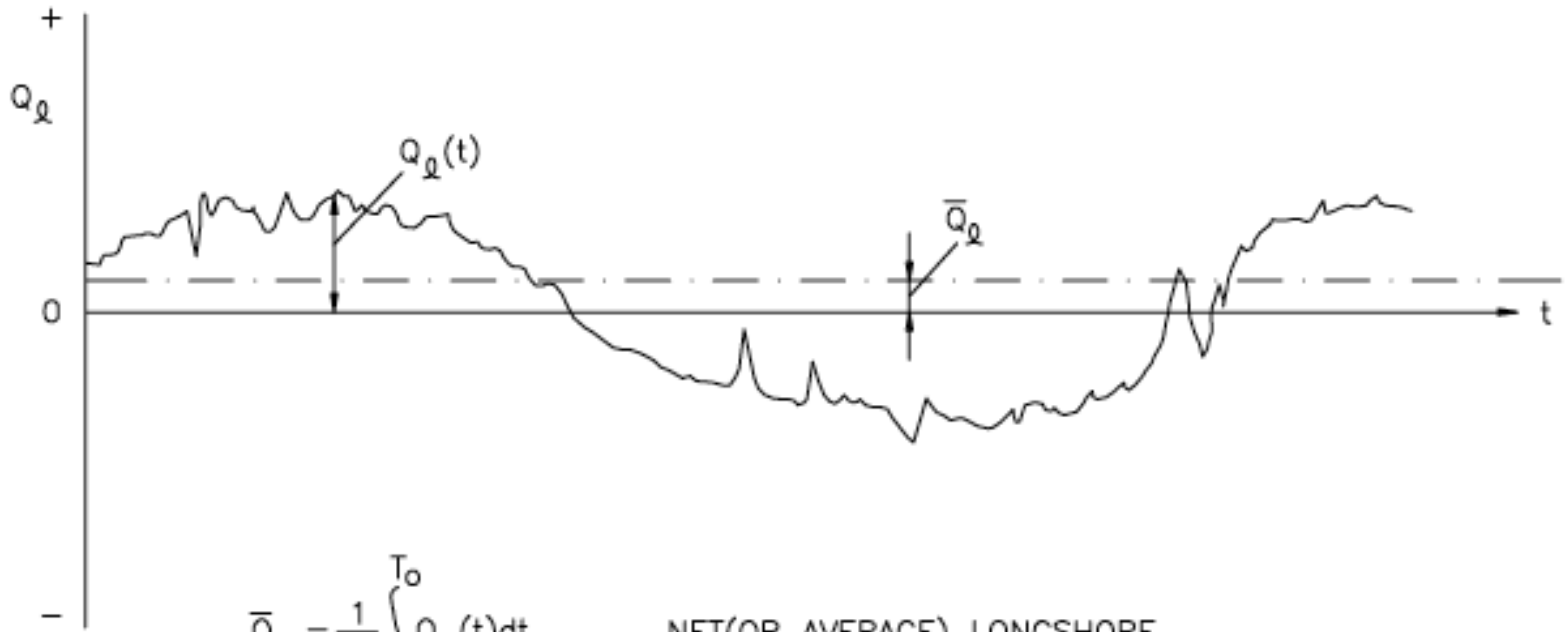

$$\overline{Q}_\ell = \frac{1}{T_o}\int_o^{T_o} Q_\ell(t)\,dt$$ NET(OR AVERAGE) LONGSHORE TRANSPORT

$$Q_{gross} = \frac{1}{T_o}\int_o^{T_o} \left| Q_\ell(t) \right| dt$$ GROSS LONGSHORE TRANSPORT

A littoral sediment budget reflects an application of the principle of **continuity or conservation of mass** to coastal sediment. The time rate of change of sediment within a system is dependent upon the rate at which material is brought into a **control volume** versus the rate at which sediment leaves the same volume.

The budget involves assessing the sedimentary contributions and losses and equating these to the net balance of sediment in a coastal compartment. Any process that results in a net increase in sediment in a control volume is called a **source**. Alternately, any process that results in a net loss of sediment from a control volume is considered a **sink**.
Some processes can function as sources and sinks for the same control volume (e.g., longshore sediment transport).

The balance of sediment between losses and gains is reflected in **localized erosion** and **deposition**. In general, longshore movement of sediment **into a coastal compartment**, *onshore transport of sediment*, additions from fluvial transport, and dune/bluff/cliff erosion provide the **major sources** of sediment.

Longshore movement of sediment **out of a coastal compartment**, *offshore transport of sediment*, and aeolian transport and washover that increase beach/island elevation produce losses from a control volume.

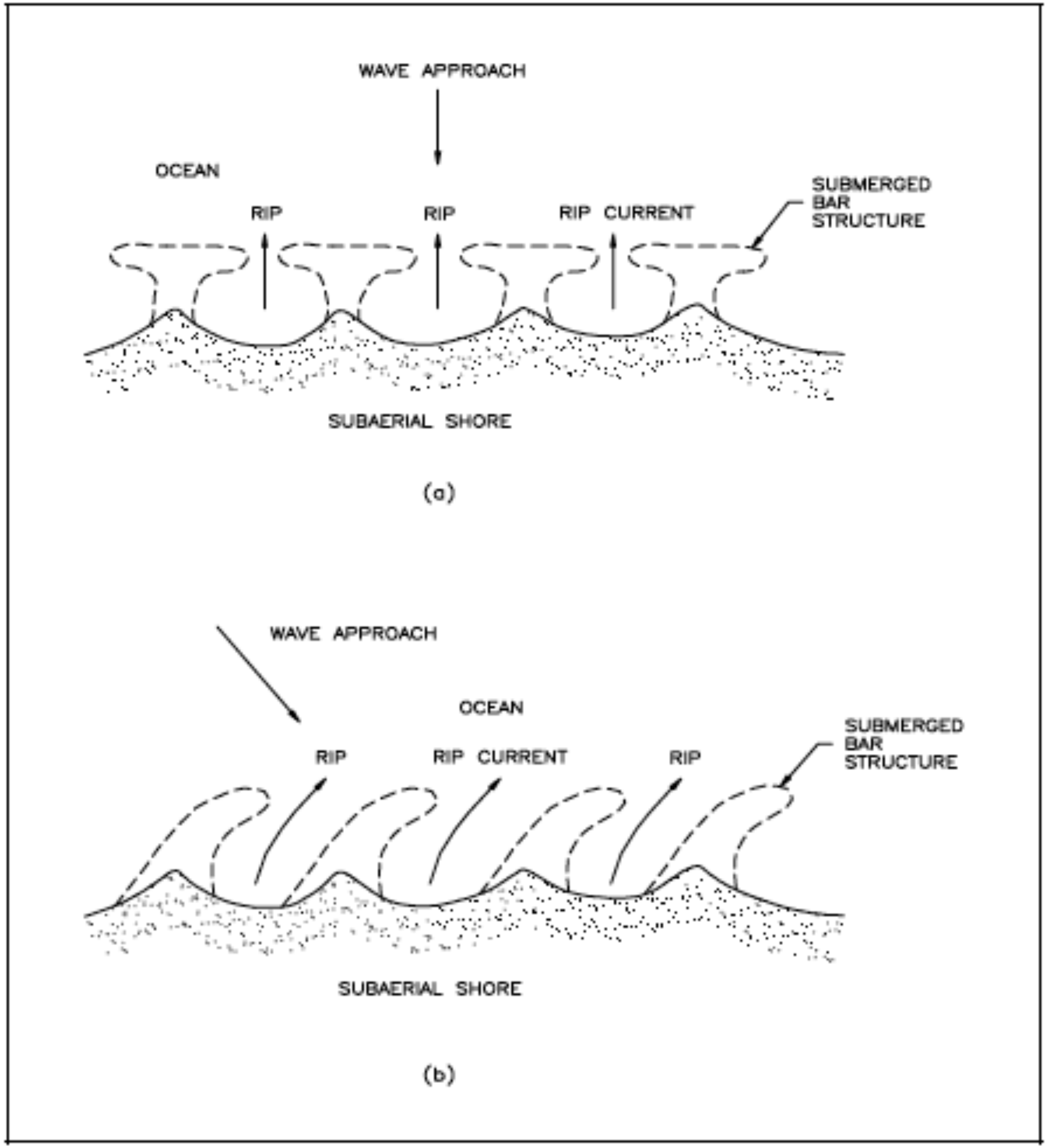
WAVE APPROACH
OCEAN
RIP
RIP
RIP CURRENT
SUBMERGED
BAR
STRUCTURE
SUBAERIAL SHORE
(a)
WAVE APPROACH
OCEAN
RIP
RIP CURRENT
RIP
SUBMERGED
BAR
STRUCTURE
SUBAERIAL SHORE
(b)

Different profile of bathimetry

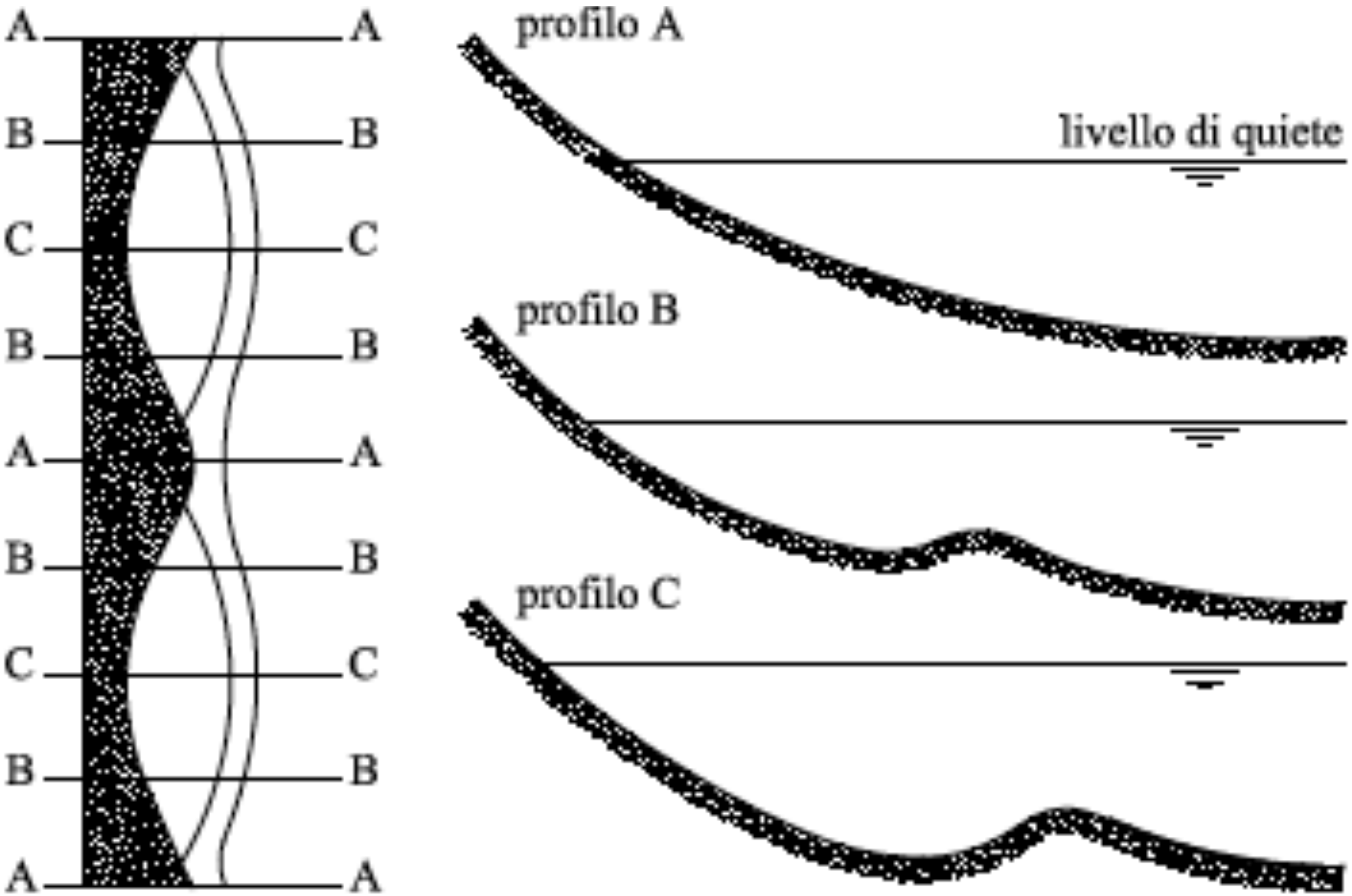

Winter and Summer profile

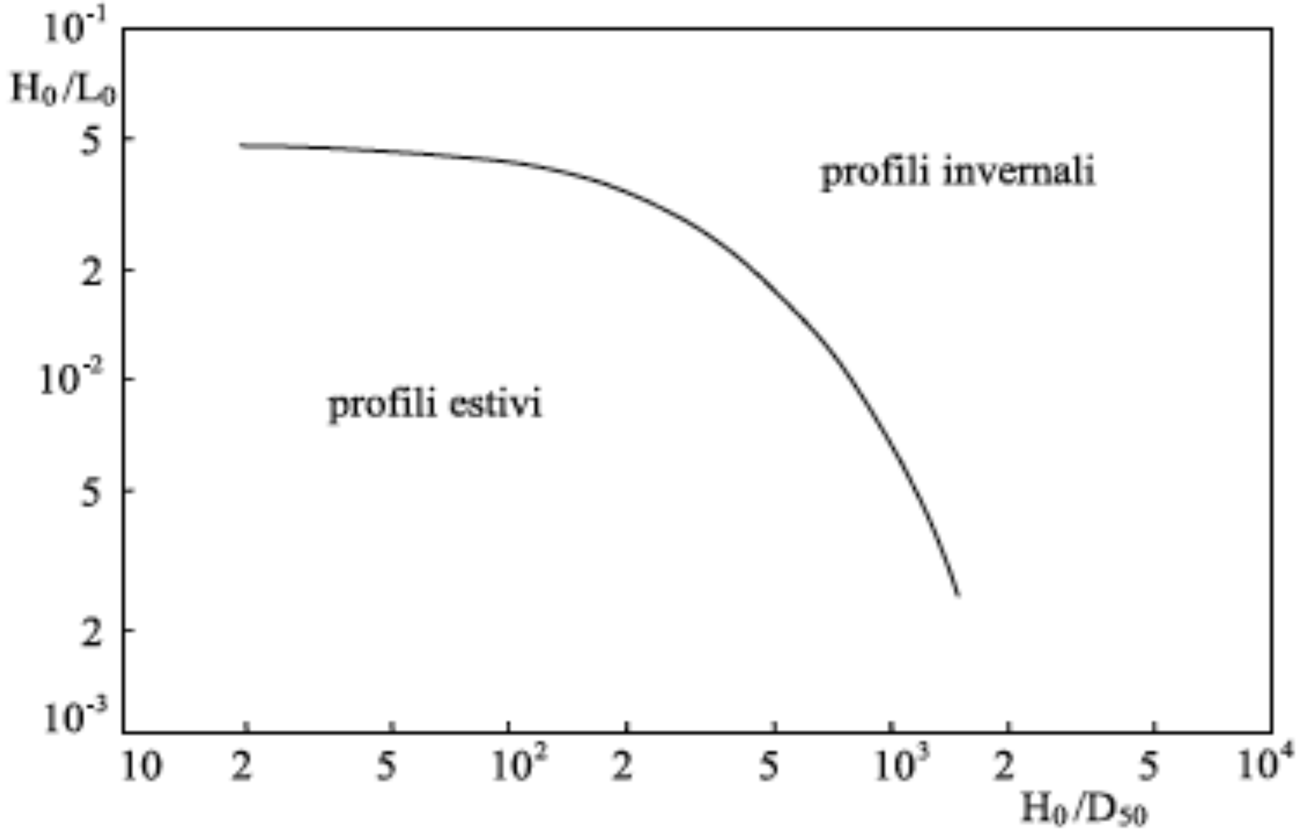

Relationship between sea condition and dimension of sediment

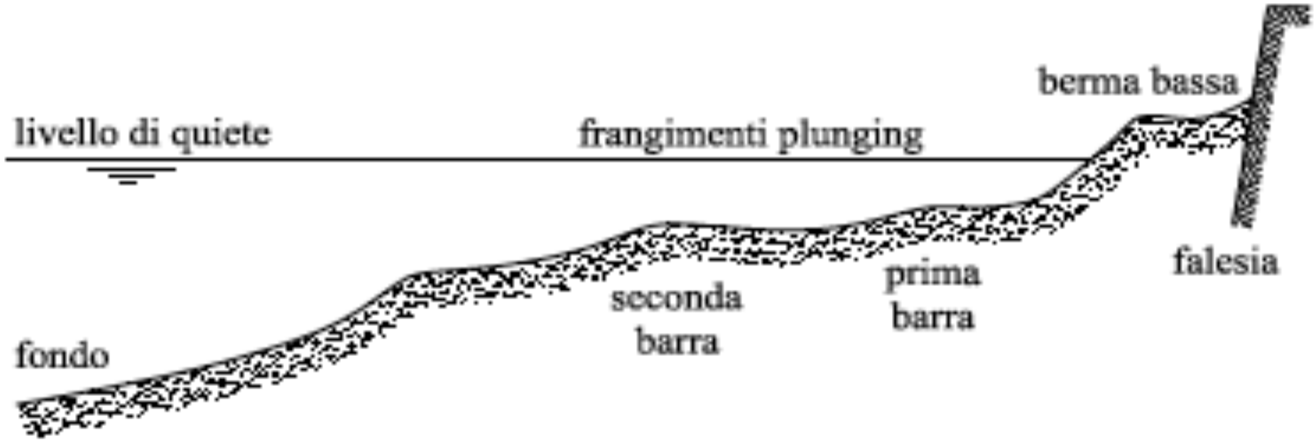

Profile in the case of dissipative beach

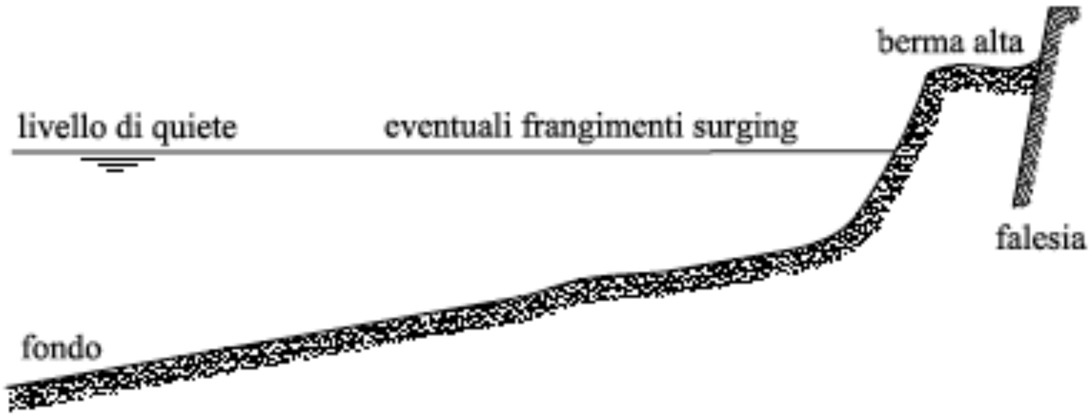

Profile in the case of reflective beach

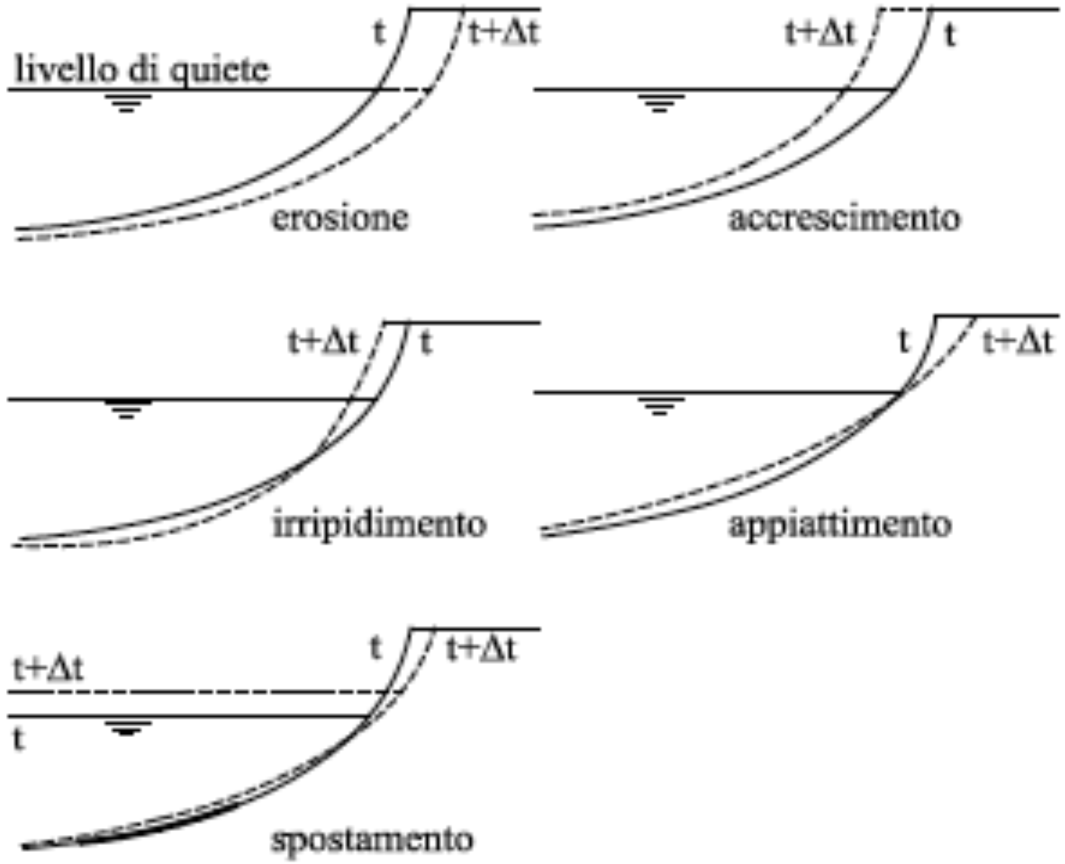

Profile in the case of no-equilibrium beach

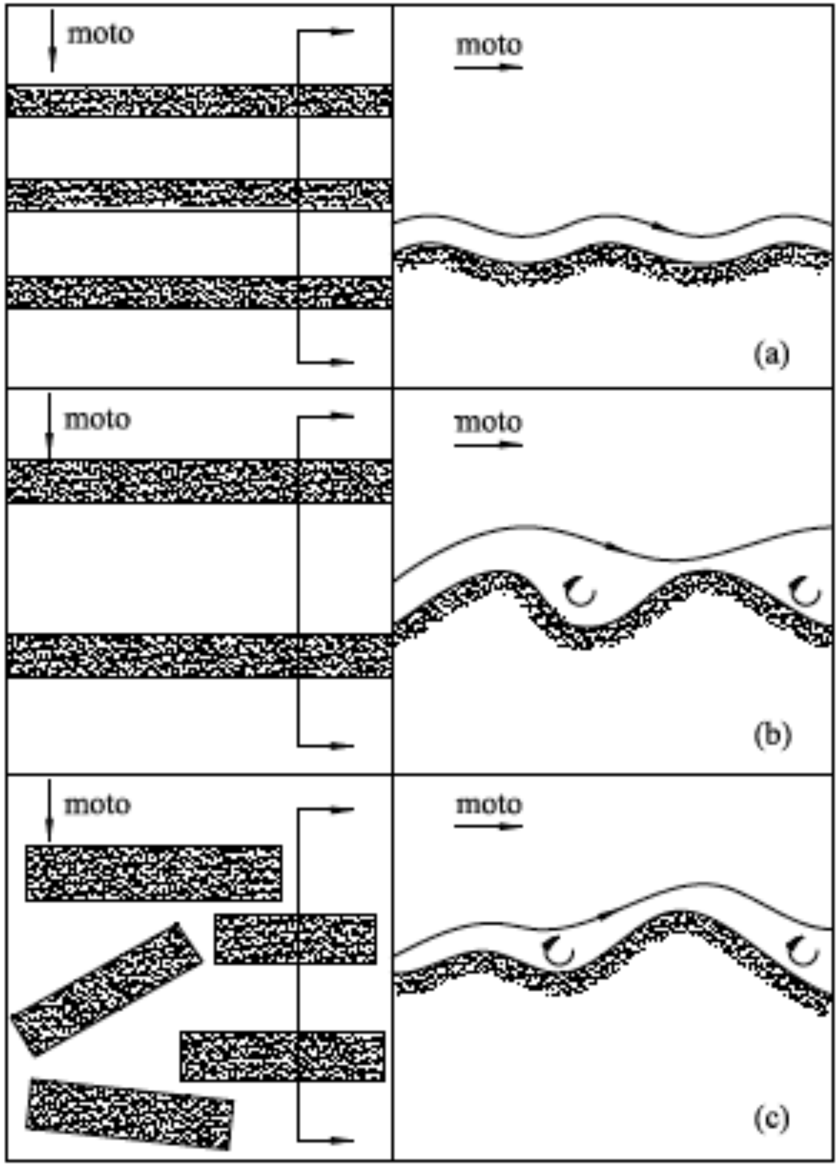

Figura 8.18. Rolling-grain ripples, (a); vortex ripples bidimensionali, (b); vortex ripples tridimensionali, (c). Rappresentazione fortemente schematica.

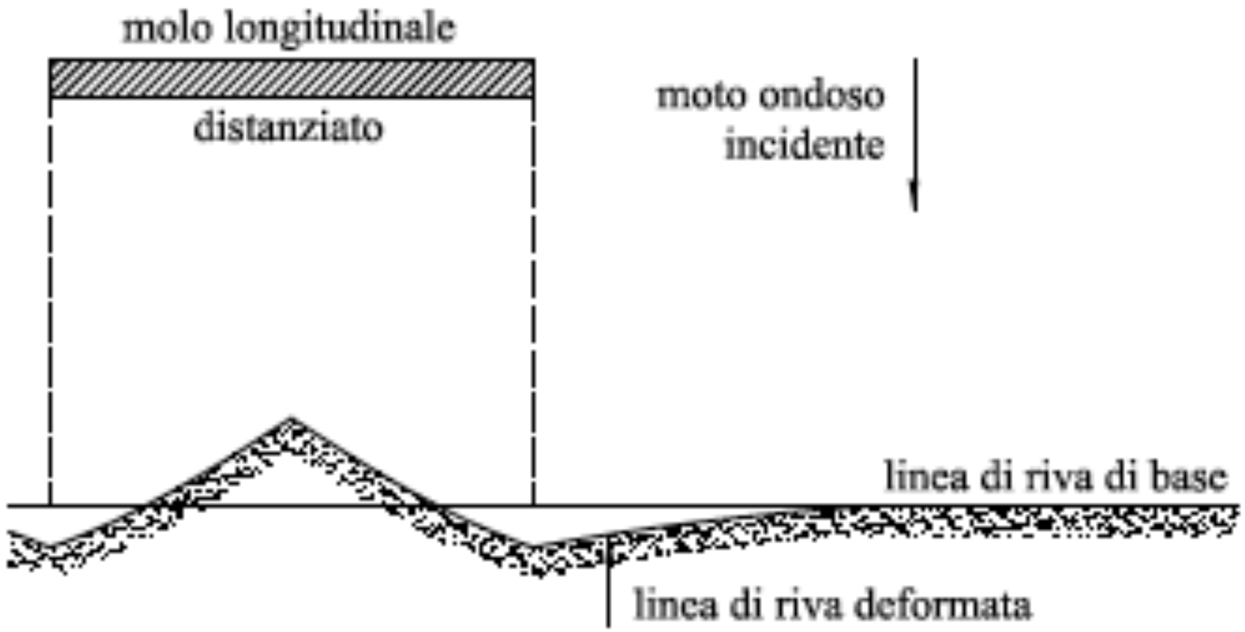
molo longitudinale
distanziato
moto ondoso
incidente
linea di riva di base
linea di riva deformata

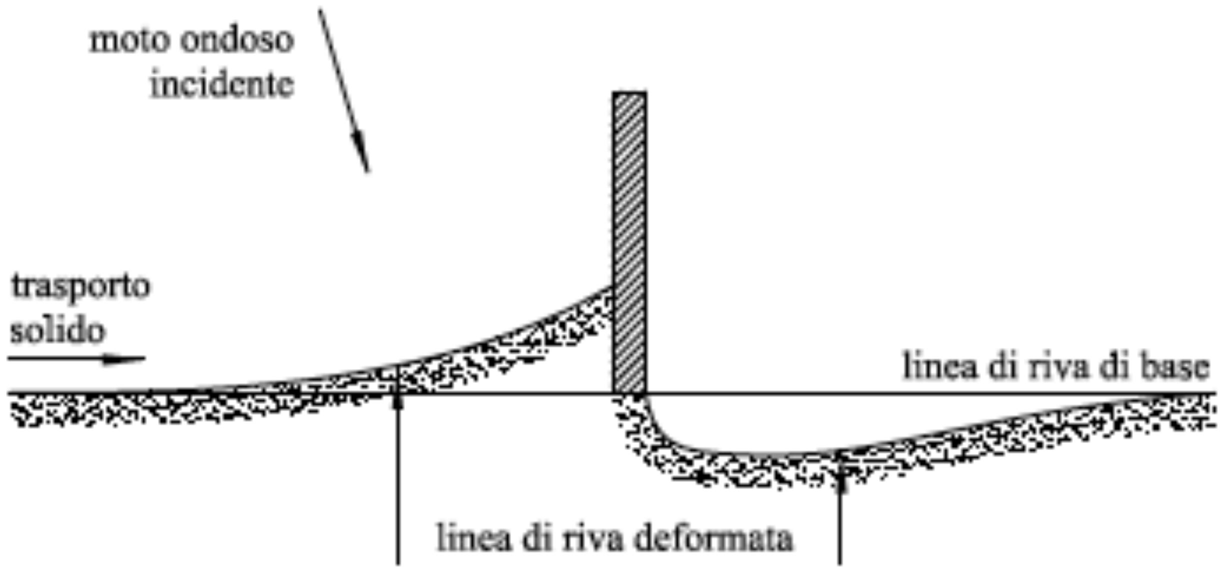
moto ondoso
incidente
trasporto
solido
linea di riva di base
linea di riva deformata


moto ondoso
incidente
linea di riva
di base
linea di riva deformata

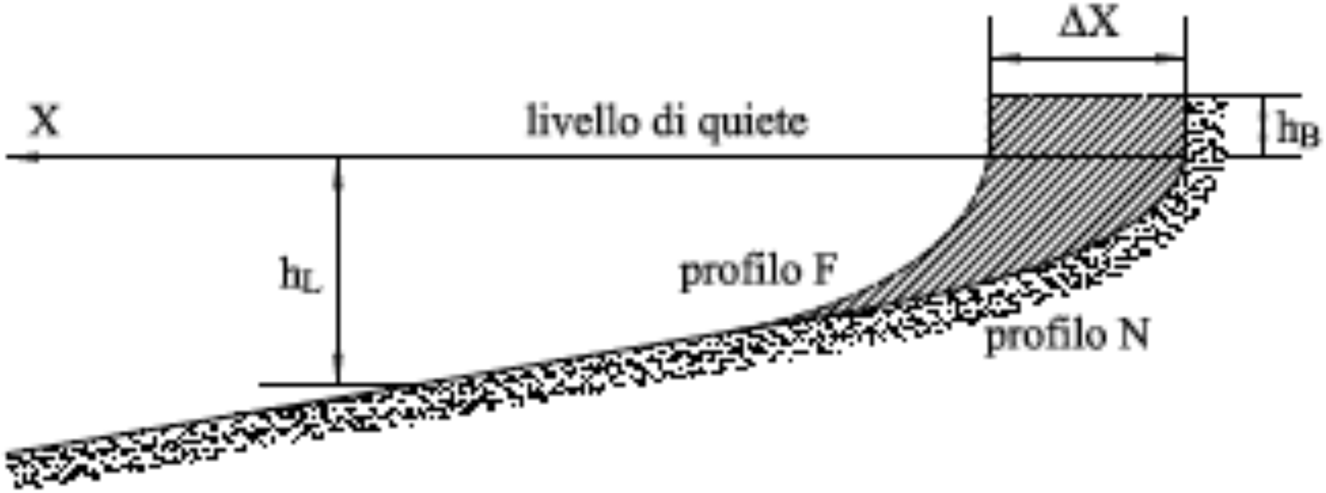

Nourishment of the beach, Profile F intersect

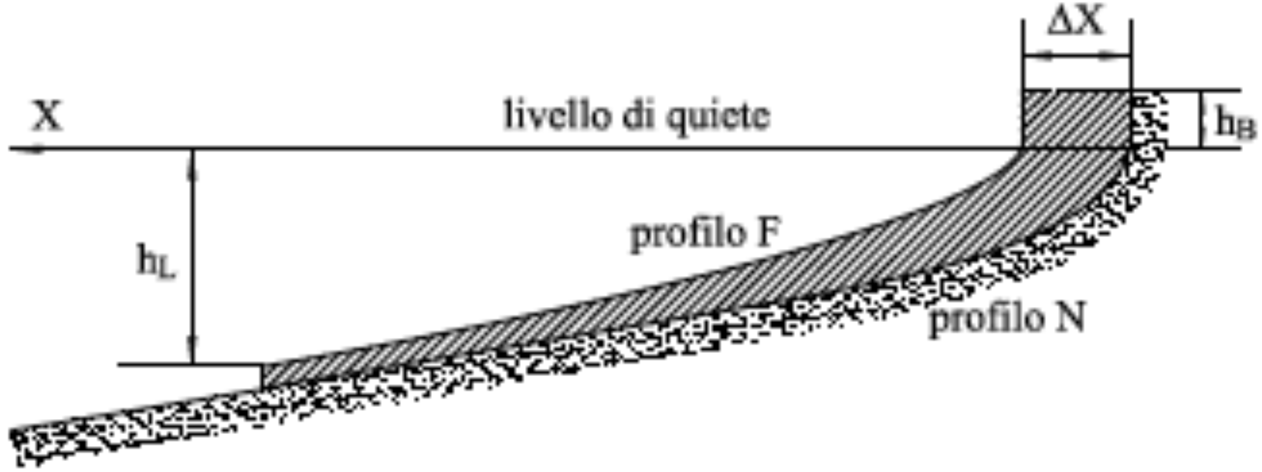

Nourishment of the beach, Profile F no intersect

Nourishment of the beach, Profile F submerged

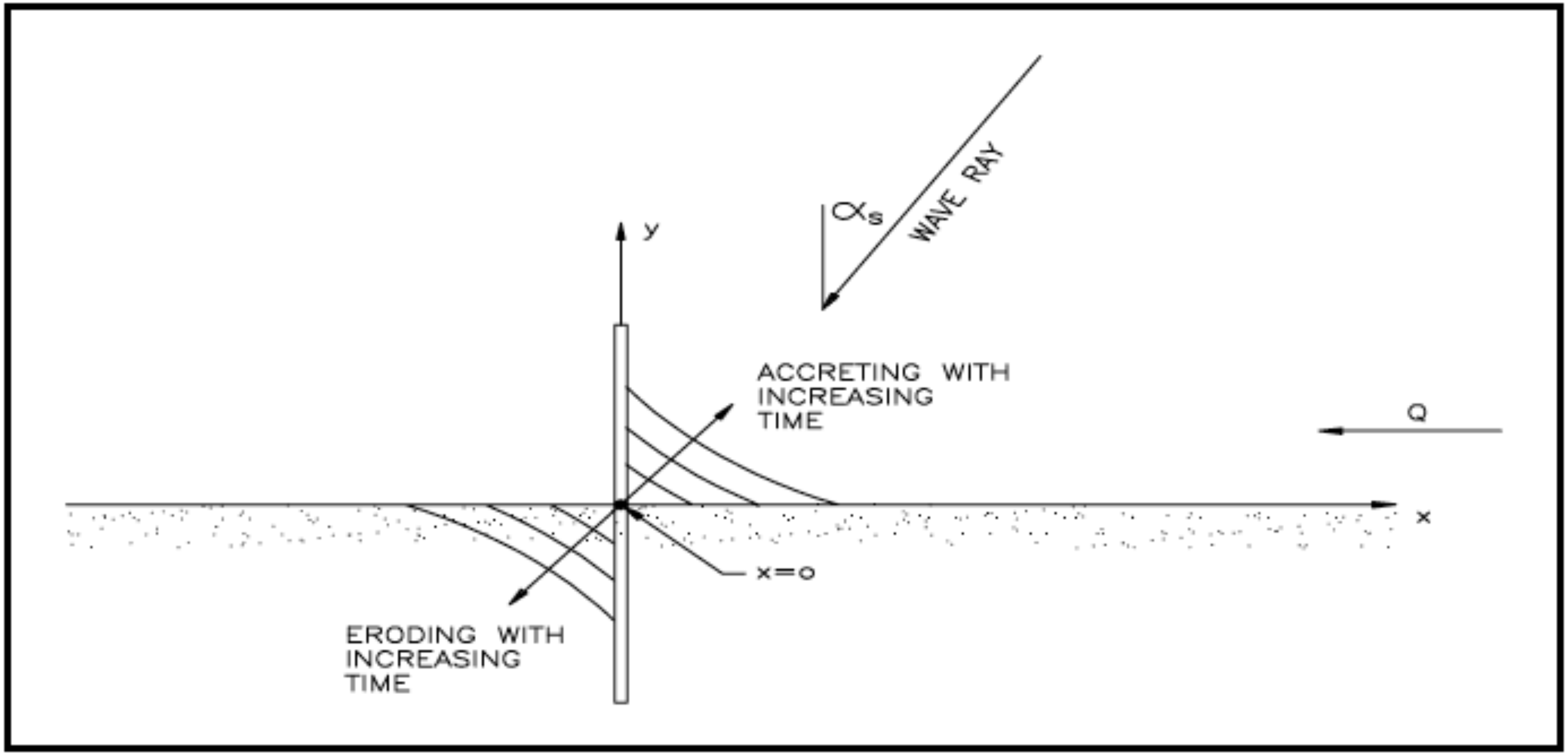
y
α_s
WAVE RAY
ACCRETING WITH
INCREASING
TIME
Q
x
x=o
ERODING WITH
INCREASING
TIME

As opposed to analytical solutions of shoreline change, which simplify the equations used to predict beach evolution**, mathematical modeling** facilitates generalization of these equations so that input parameters may vary **in time and in the longshore, and possibly cross-shore, dimensions.**

Numerical models of beach change perform best when a perturbation is introduced to a system that is in *equilibrium*.

The perturbation to the system might be an introduction or removal of littoral material (e.g., beach fill, sand mining, release of sediment due to a flooded river or landslide) or placement of a hardened structure (e.g., groins, detached breakwaters, seawalls, revetments).

Historical trends of beach change and knowledge of the littoral budget are typically used to **calibrate and verify** the controlling equations, then forecasts may be simulated as a function of various engineering alternatives and/or wave climate scenarios.

Therefore, beach response as a function of complex coastal processes may be readily examined in detail with mathematical models.

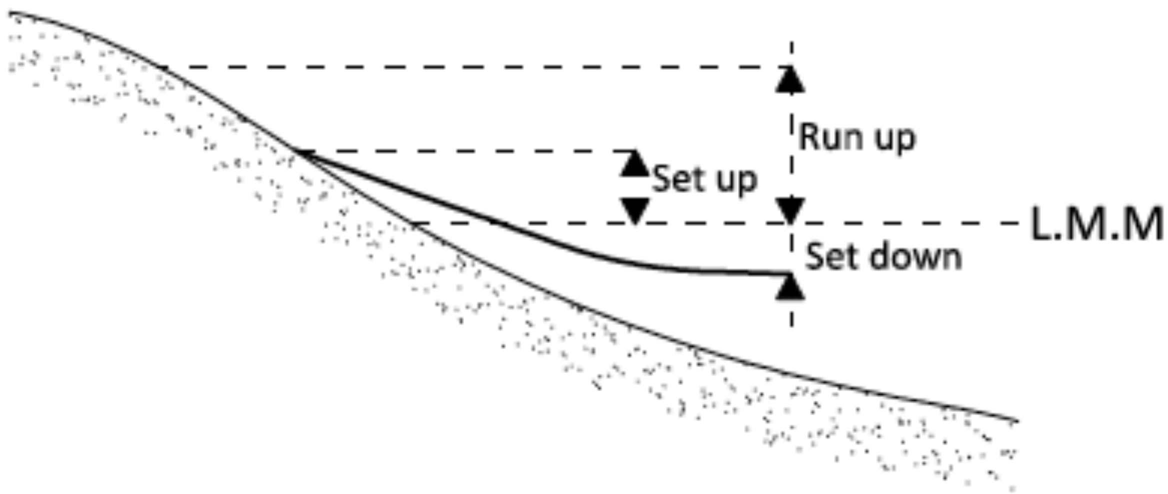

Run up
Set up
L.M.M
Set down

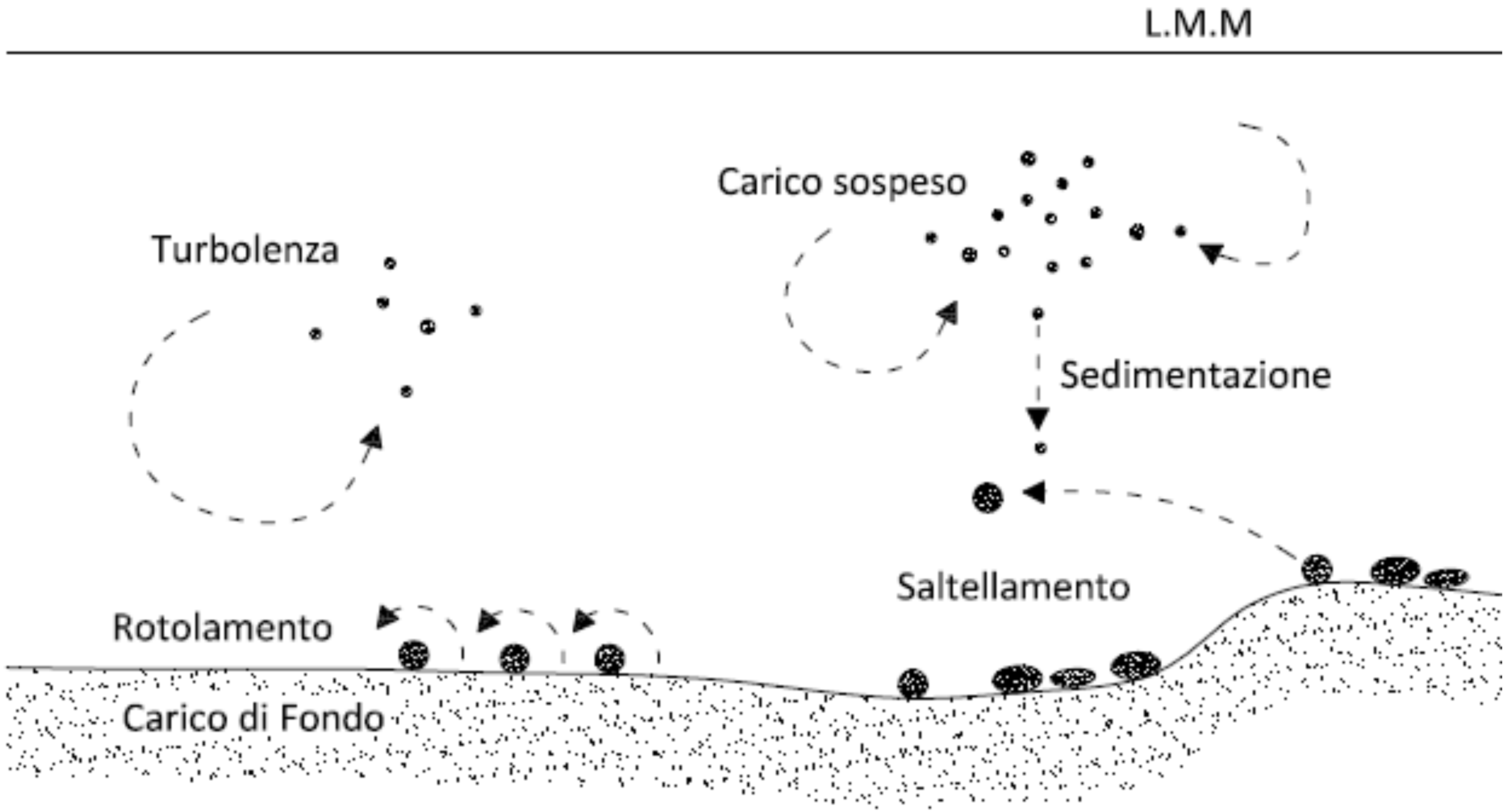
L.M.M
Carico sospeso
Turbolenza
Sedimentazione
Saltellamento
Rotolamento
Carico di Fondo

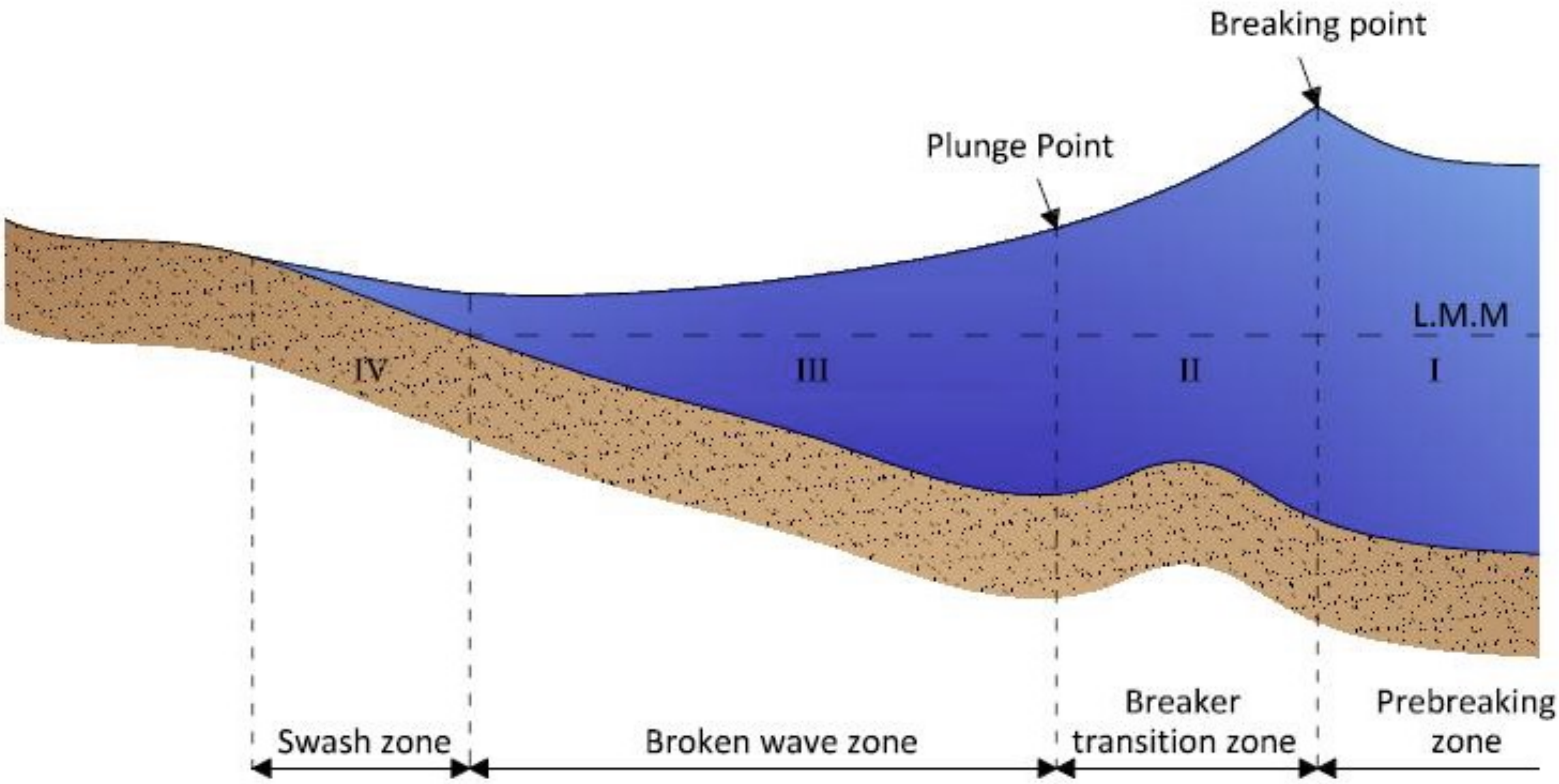
Breaking point
Plunge Point
L.M.M
IV
III
II
I
Swash zone
Broken wave zone
Breaker transition zone
Prebreaking zone

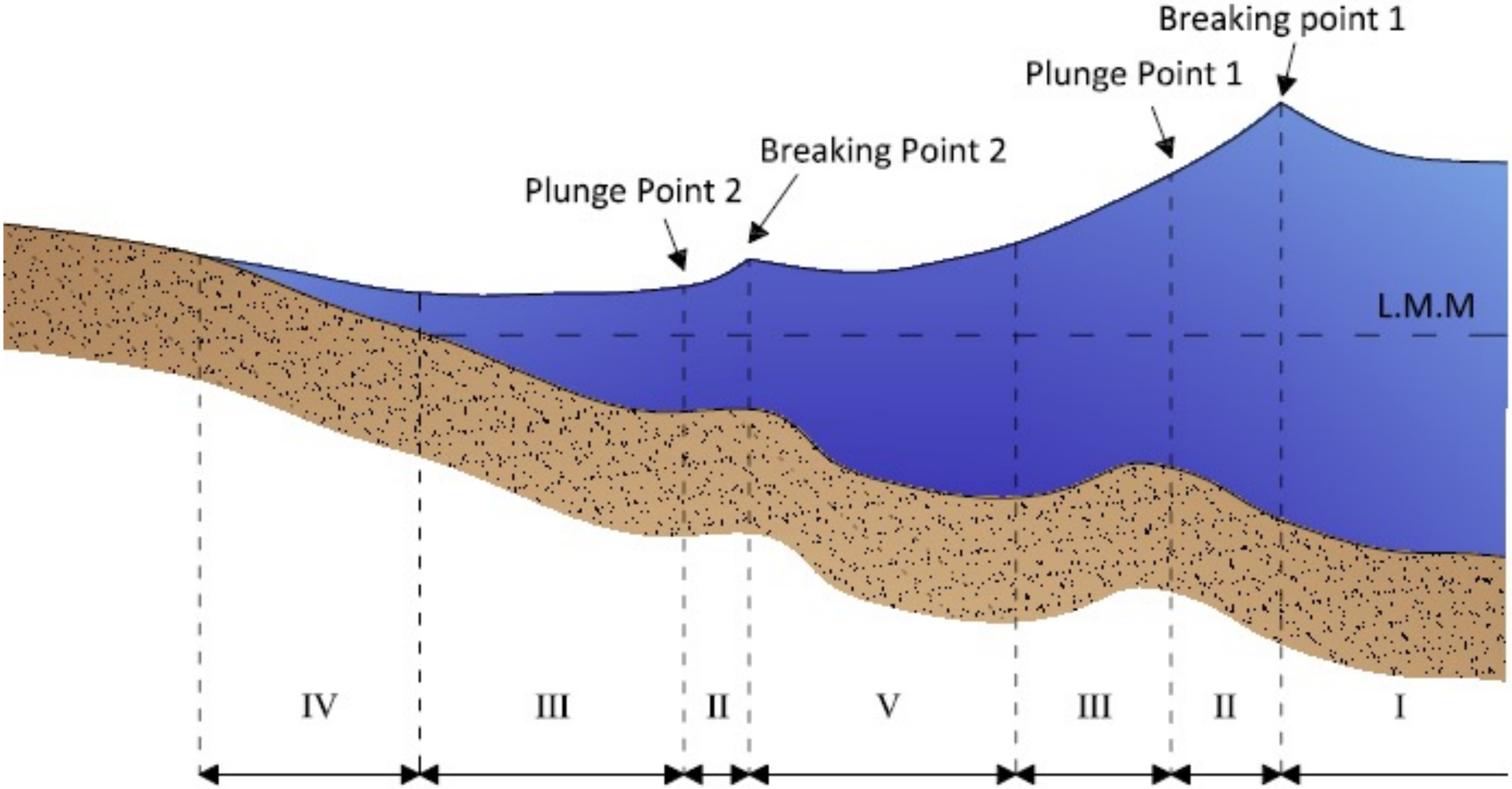
Breaking point 1
Plunge Point 1
Breaking Point 2
Plunge Point 2
L.M.M
IV
III
II
V
III
II
I

Avalanche phenomen
Transport offshore or onshore

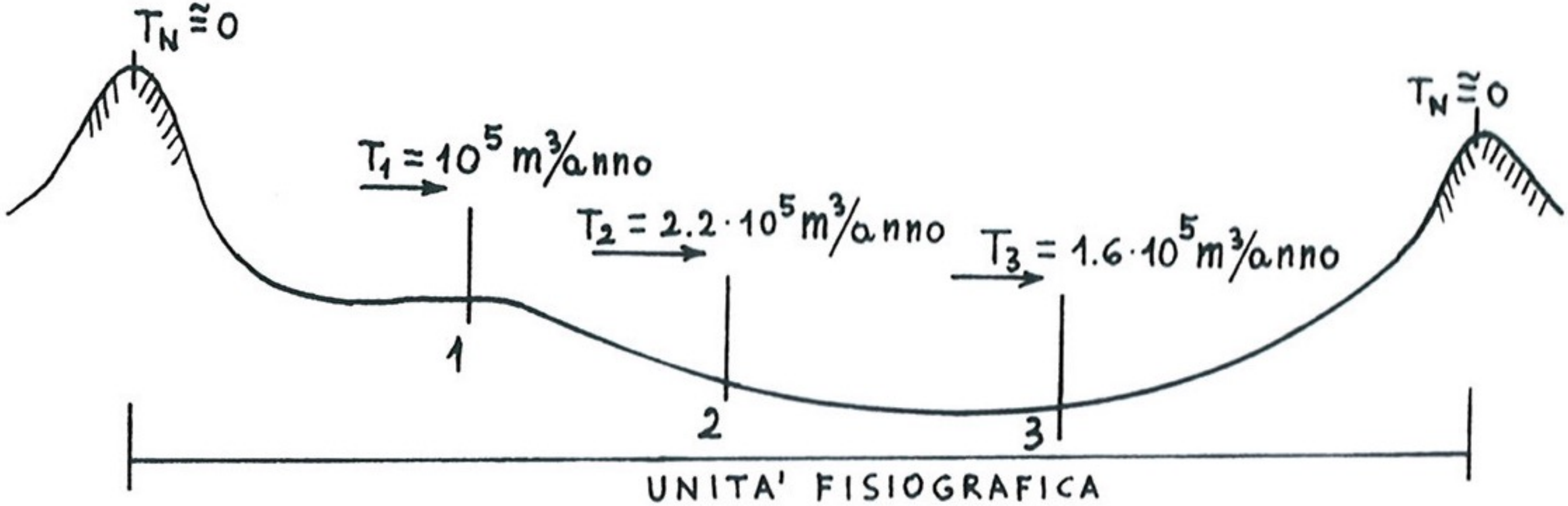

Figura 10.4 – *Perdite e accumuli di sedimenti per effetto della variazione del trasporto longitudinale netto*

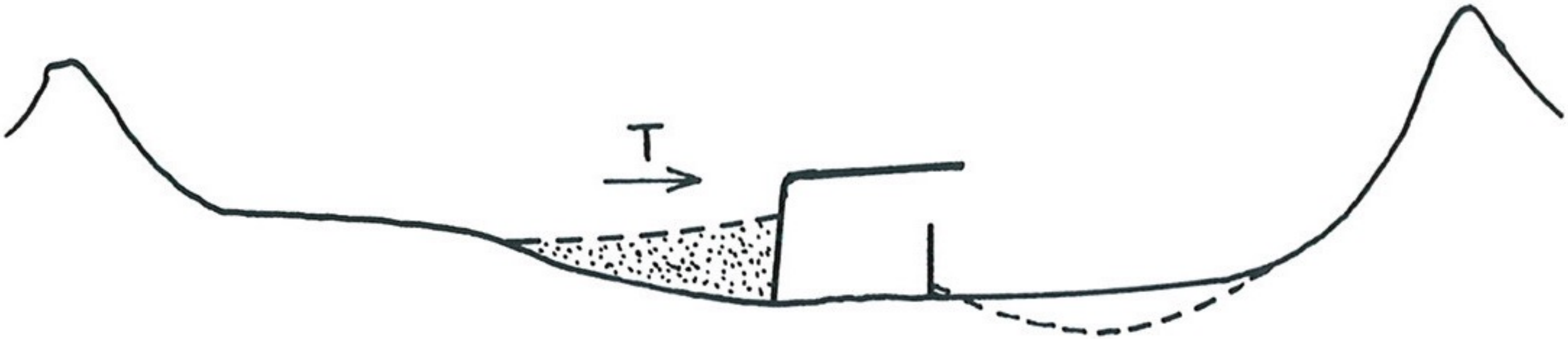

Figura 10.5 – *Variazione brusca del trasporto longitudinale netto per la presenza di un porto, con conseguenti fenomeni di erosione del litorale sottoflutto e di avanzamento del litorale sopraflutto*

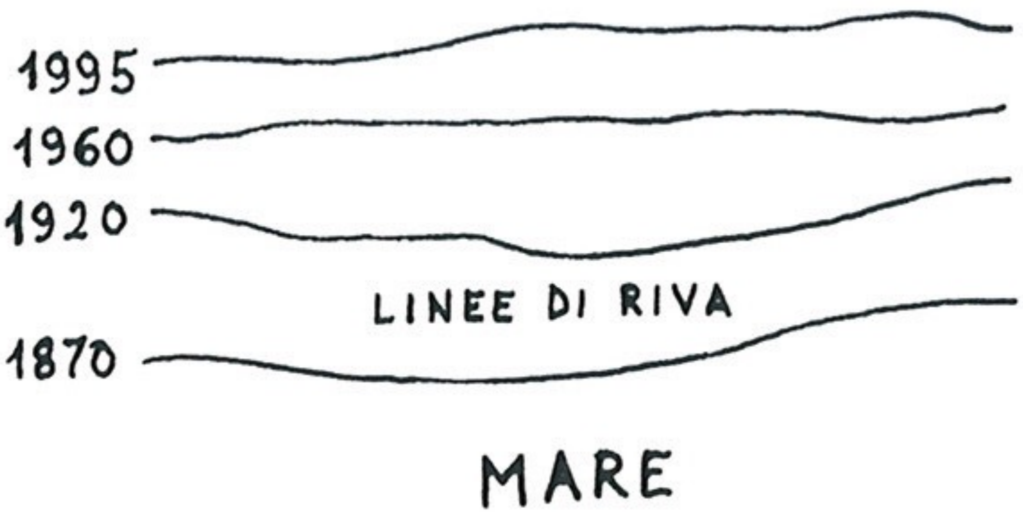

Figura 10.6 – *Arretramenti regolari della linea di riva dovuti verosimilmente a cause naturali*

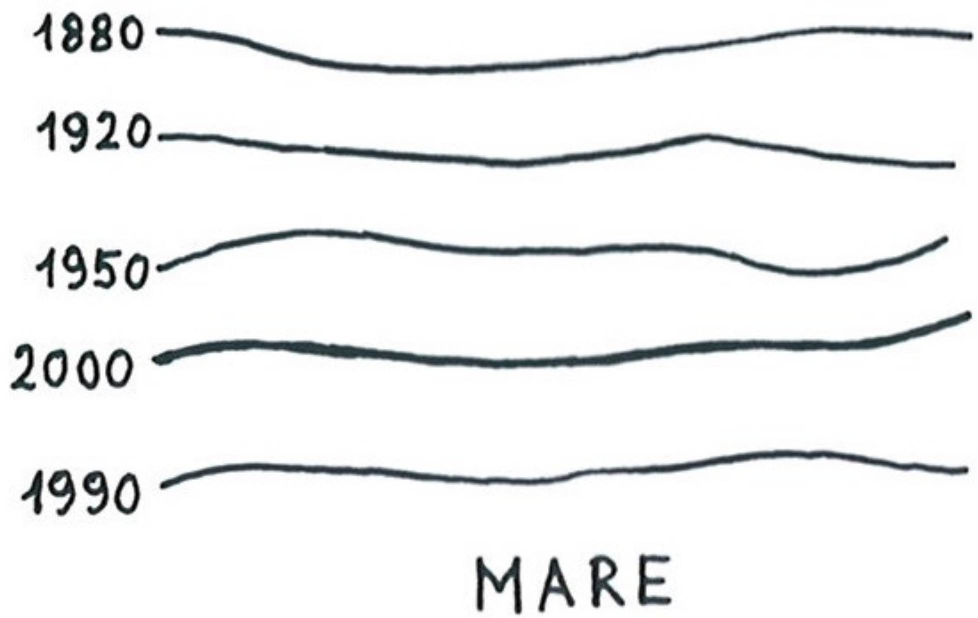

Figura 10.7 – *Arretramento recente della linea di riva dovuto verosimilmente a cause antropiche*

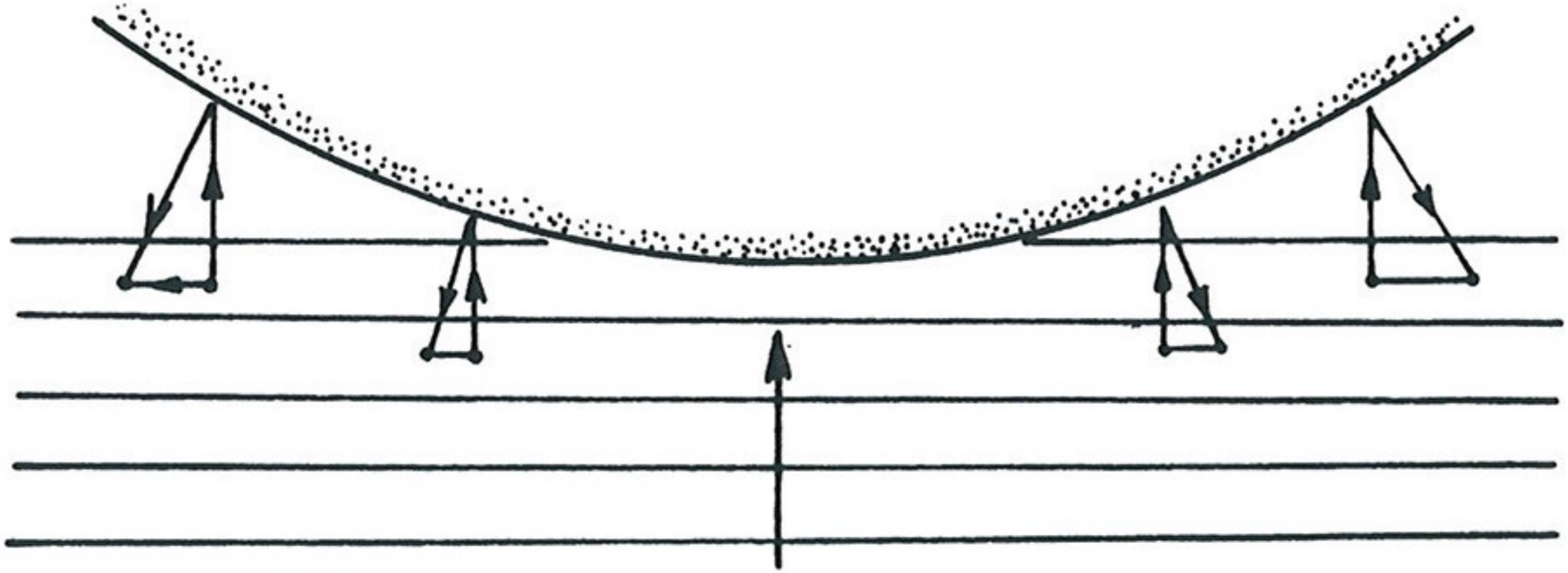

10.8 – *Naturale tendenza alla rettificazione di una linea di riva convessa verso il mare*

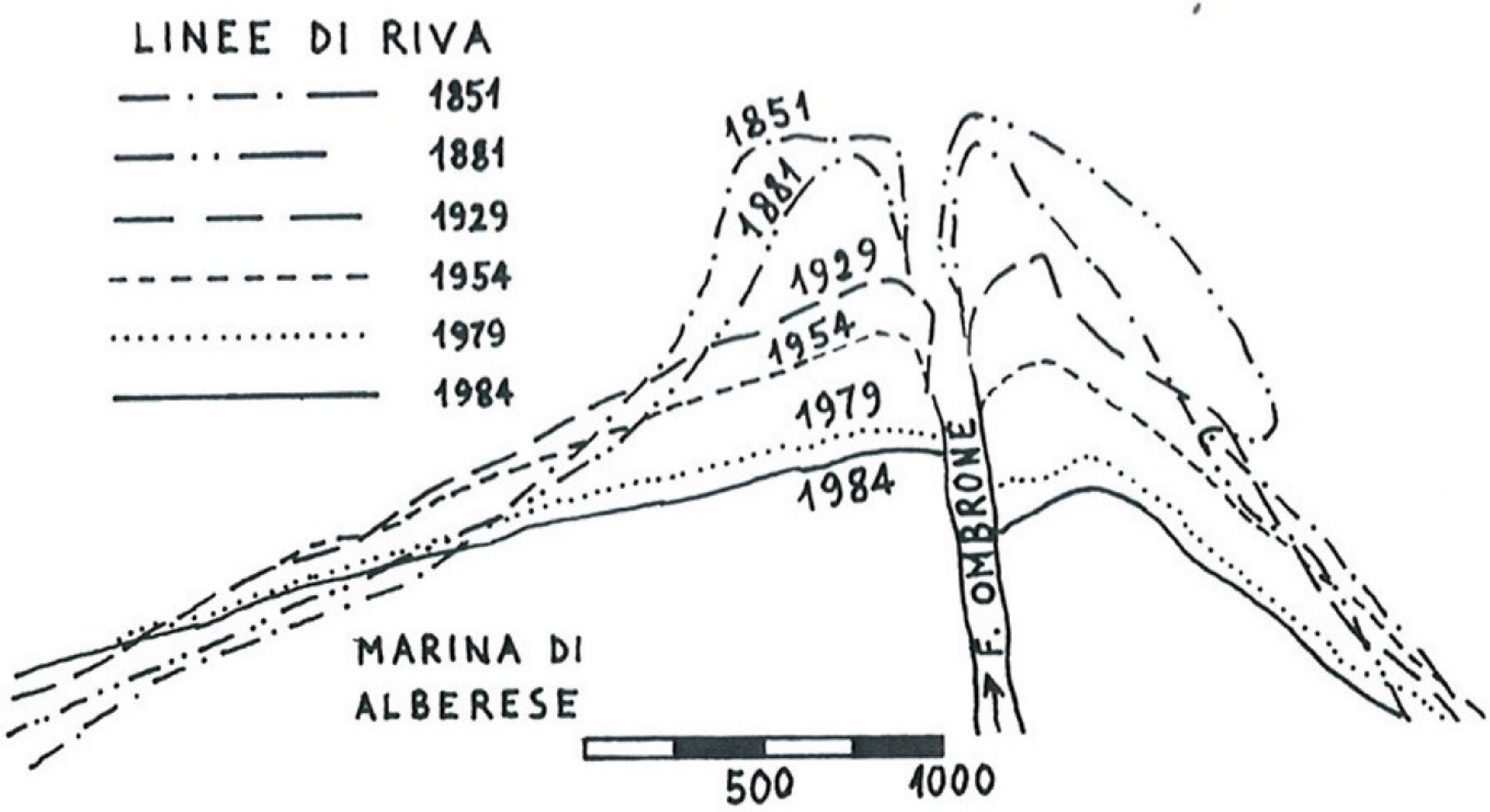

Figura 10.9 – *Forti arretramenti della linea di riva alla foce dell'Ombrone*

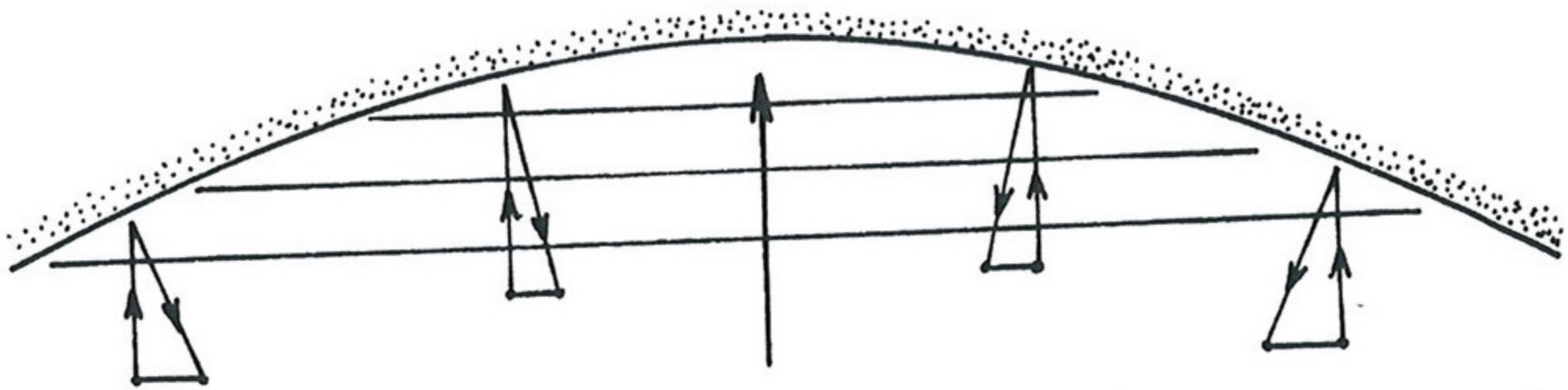

Figura 10.10 – *Naturale tendenza alla rettificazione di una linea di riva concava verso il mare*

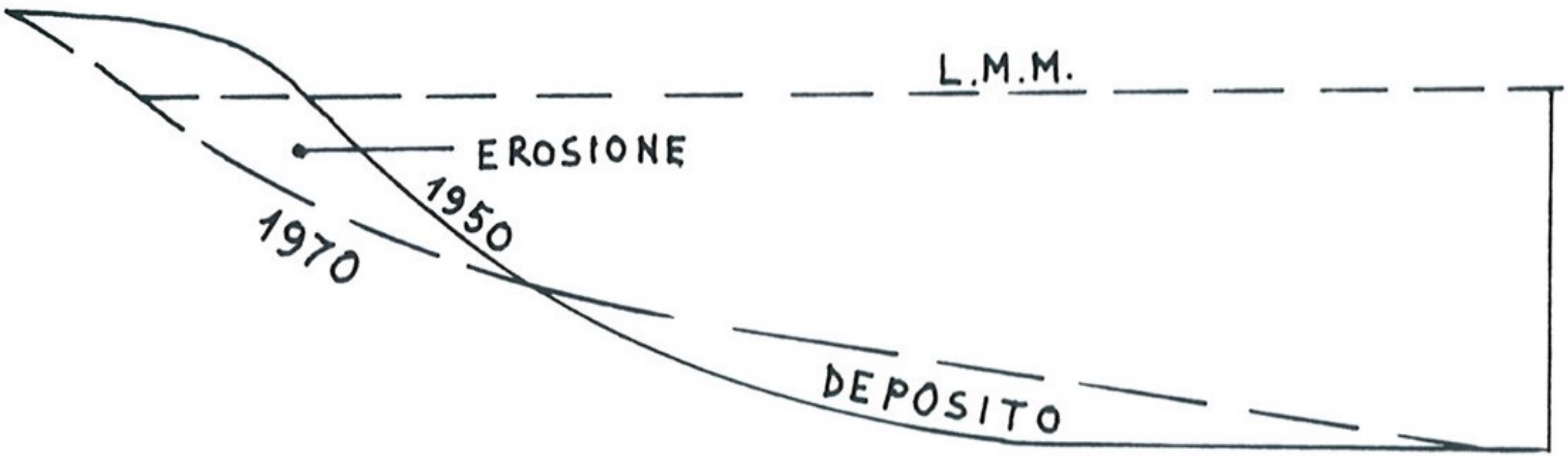

Figura 10.11 – *Sezione trasversale con arretramento della linea di riva ed erosione in bassi fondali e con deposito dei sedimenti in fondali un po' più elevati*

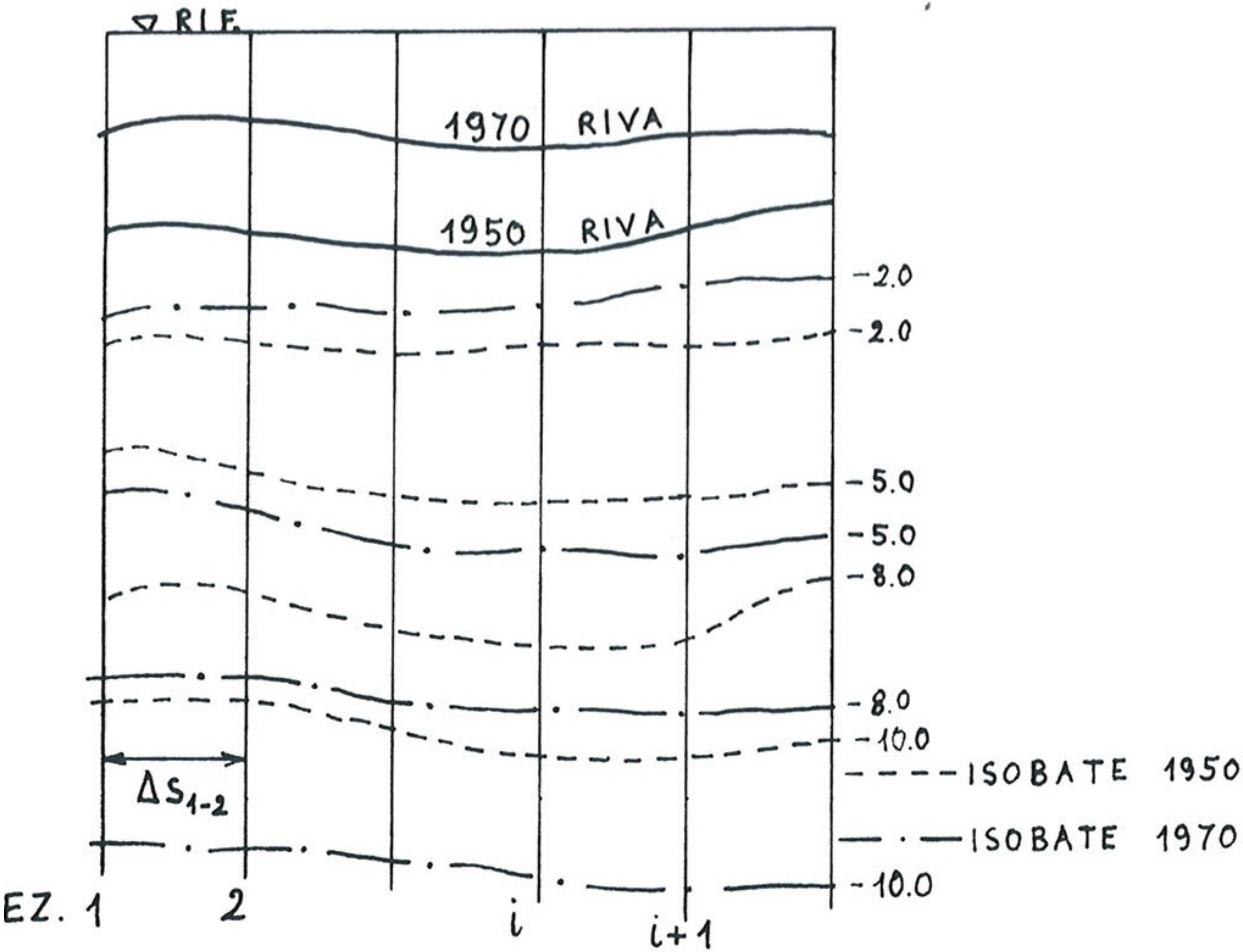

gura 10.12 – *Rilievi batimetrici all'inizio e alla fine di un determinato periodo*

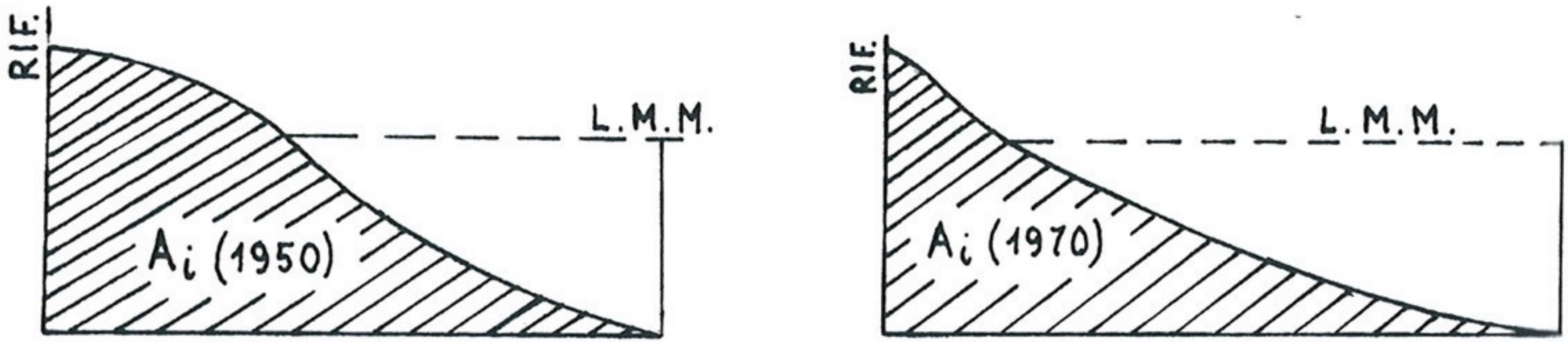

Figura 10.13 – *Sezioni trasversali all'inizio e alla fine di un determinato periodo*

$$\Delta V_{tot} = \sum_{1}^{n-1} \left(\frac{\Delta A_i + \Delta A_{i+1}}{2} \right) \Delta s_{i-i+1} \qquad (10.3)$$

essendo $\Delta A_i = A_i' - A_i$ (figura 10.14).

Figura 10.14 – *Variazioni dei sedimenti di una sezione trasversale tra l'inizio e la fine di un determinato periodo*

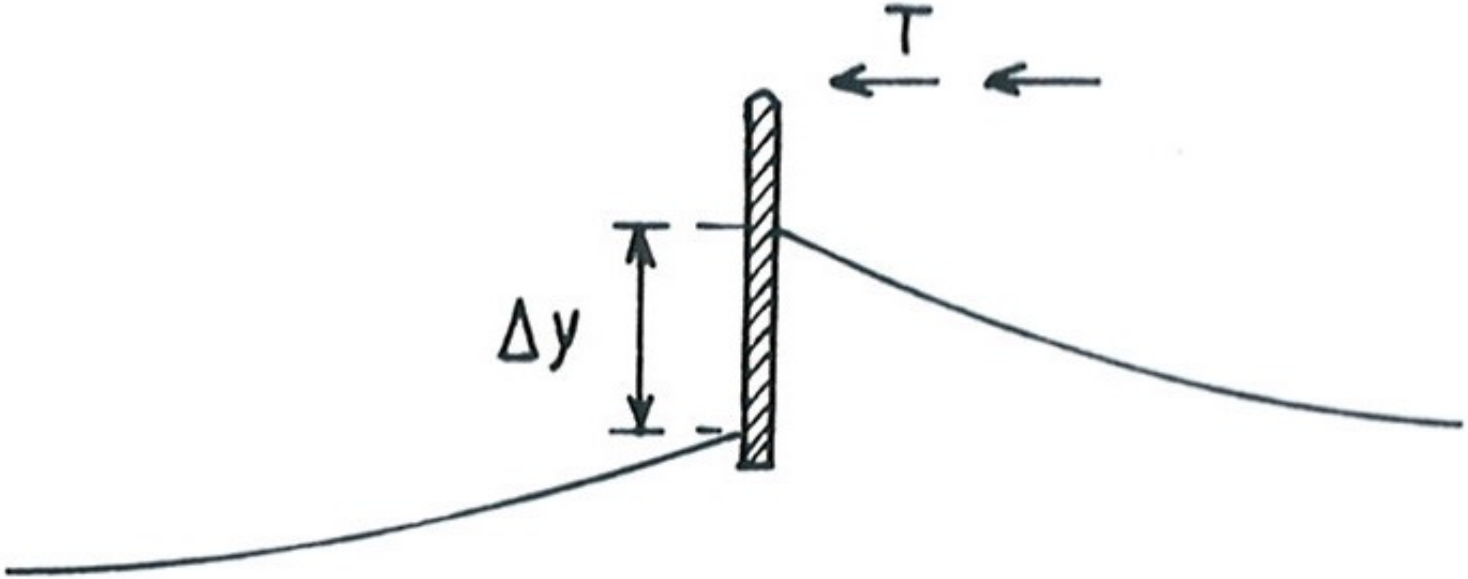

Figura 10.15 – *Discontinuità dell'andamento della linea di riva in presenza di opere trasversali*

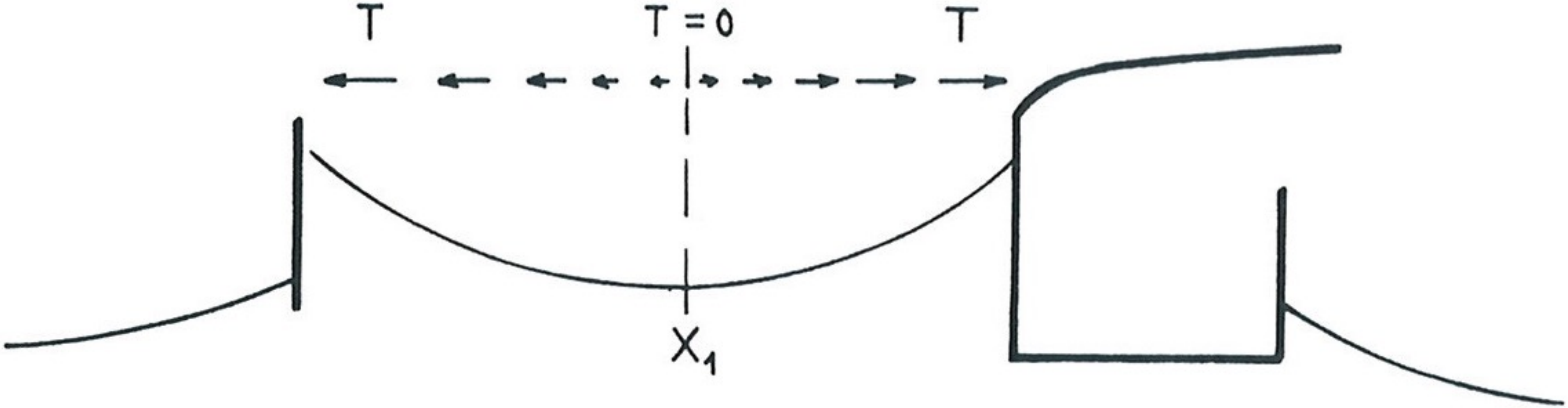

Figura 10.16 – *Presenza di una zona neutra con divergenza del senso del trasporto longitudinale netto*

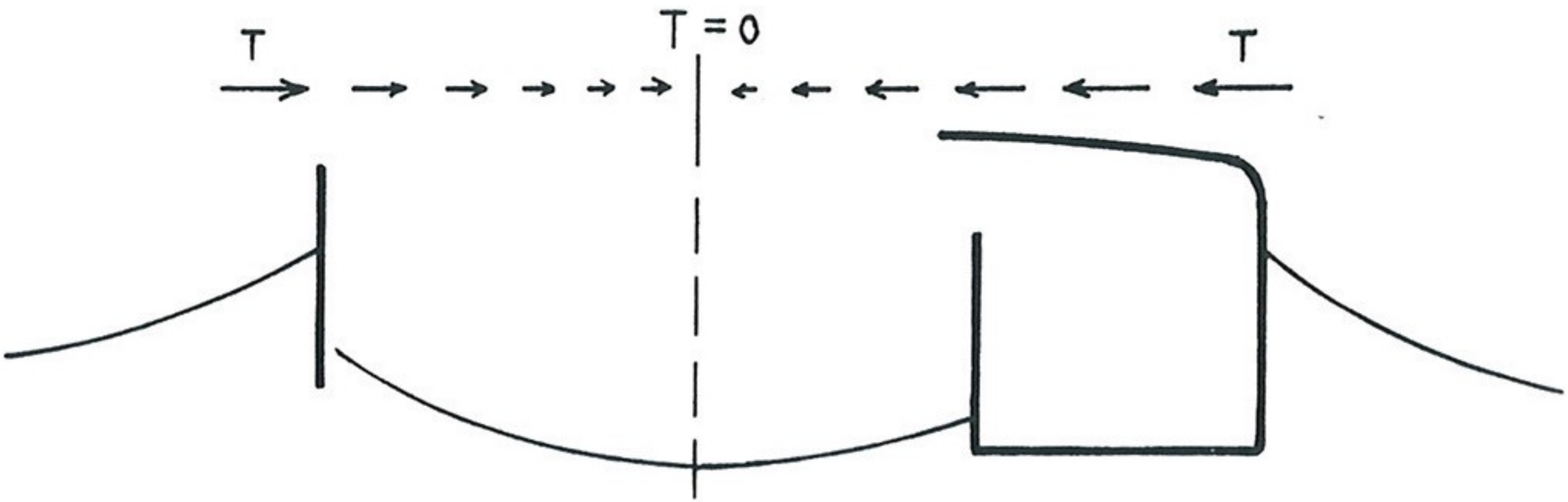

Figura 10.17 – *Presenza di una zona neutra con convergenza del senso del trasporto longitudinale netto*

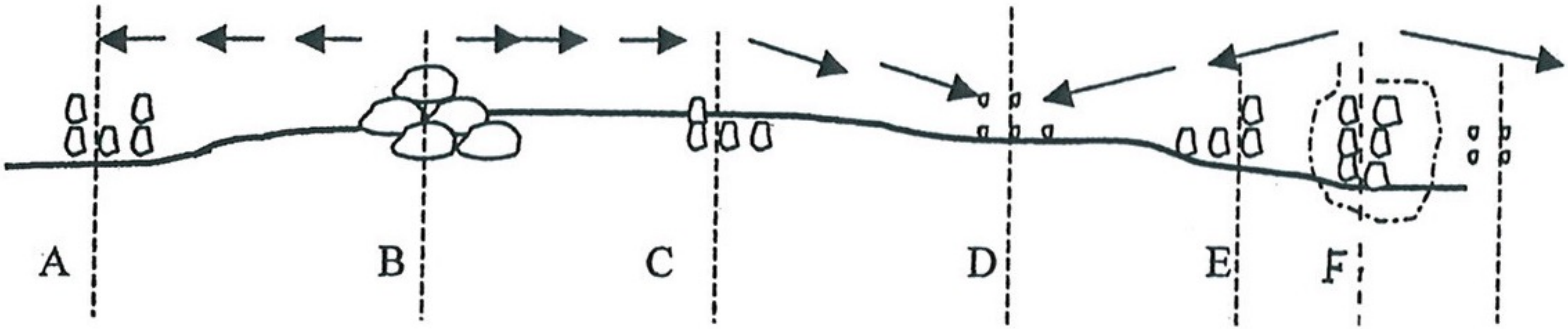

Figura 10.19 – *Andamento del senso del trasporto longitudinale netto lungo un tratto di litorale, dedotto da analisi granulometriche dei sedimenti*

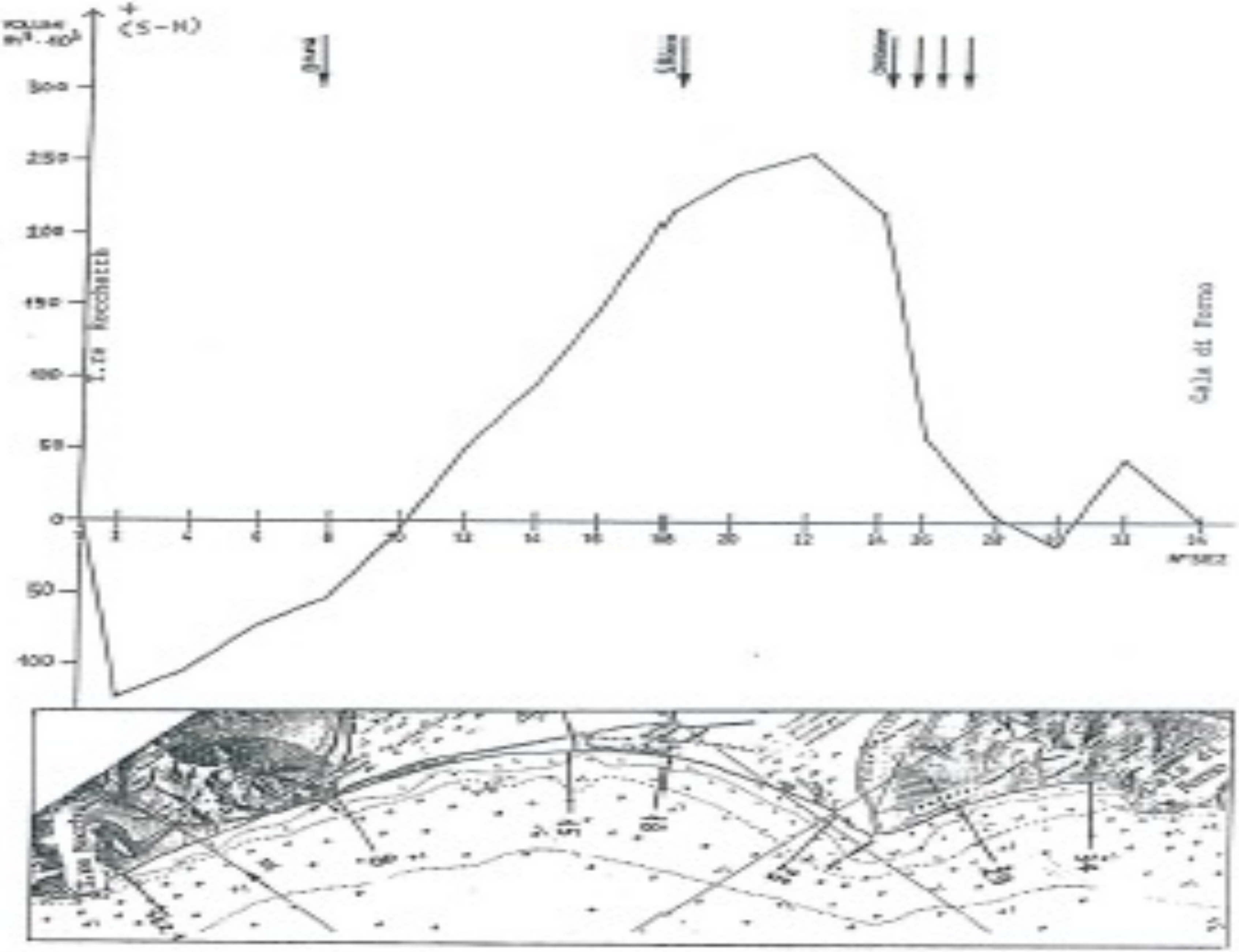

Figura 10.26 – *Andamento del trasporto longitudinale netto nel litorale tra P.ta Rocchette e Cala di Forno, determinato in funzione del clima marittimo*

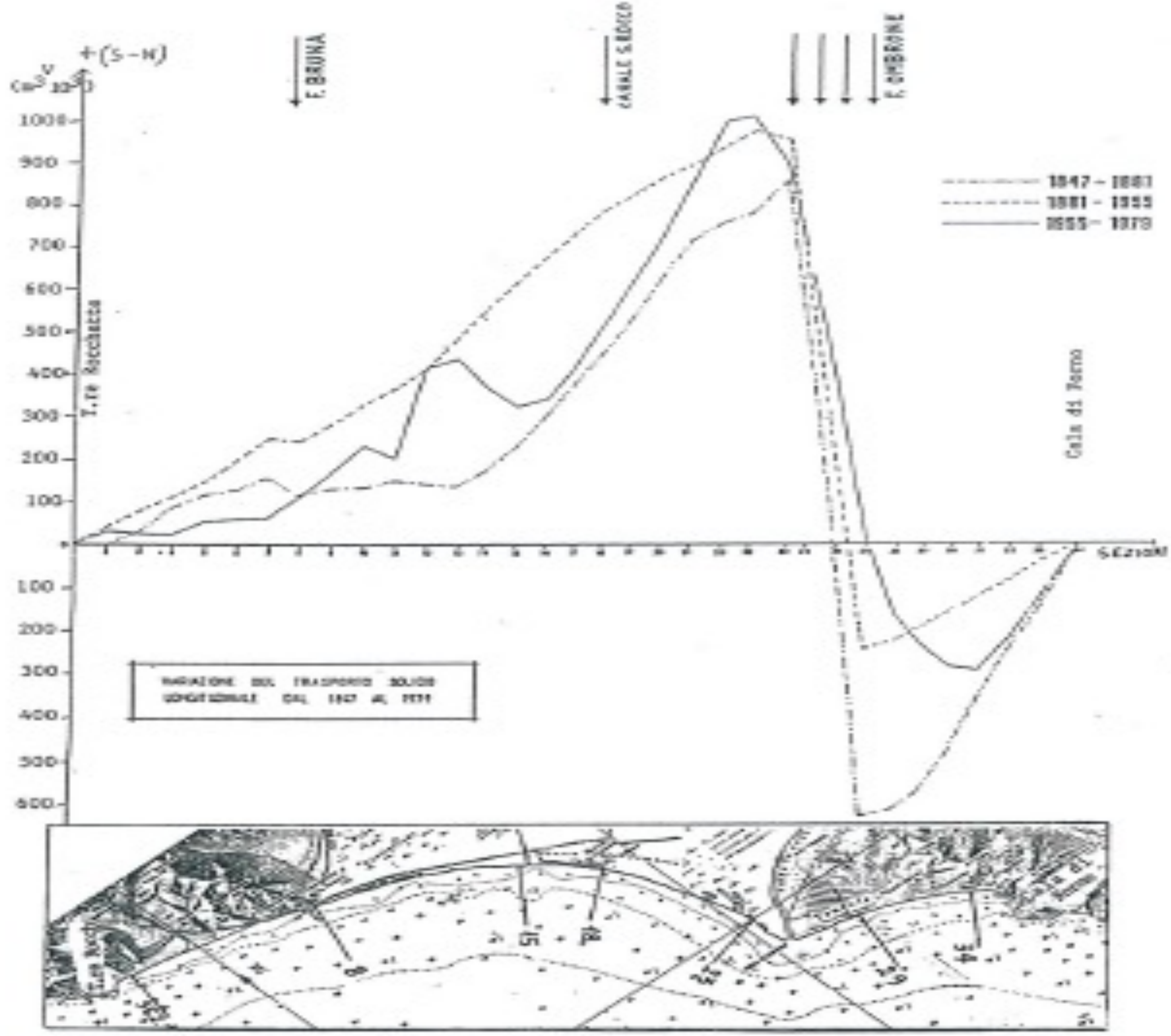

Figura 10.28 – *Andamento del trasporto longitudinale netto nel litorale tra P.ta Rocchette e Cala di Forno, in tre diversi periodi, determinato in base a rilievi batimetrici e a dati sperimentali*

International Journal of Disaster Risk Reduction 23 (2017) 45–52

Contents lists available at ScienceDirect

International Journal of Disaster Risk Reduction

journal homepage: www.elsevier.com/locate/ijdrr

Assessing Mozambique's exposure to coastal climate hazards and erosion

Pedro Cabral[a,*], Gabriela Augusto[a], Adeoluwa Akande[a], Anjos Costa[a,b], Nelson Amade[a,b], Sérgio Niquisse[a,b], Ali Atumane[a,b], António Cuna[a,b], Kiana Kazemi[a], Ramires Mlucasse[a,b], Rubini Santha[a]

[a] NOVA IMS, Universidade Nova de Lisboa, 1070-312, Portugal
[b] Universidade Católica de Moçambique, Beira, Moçambique

ARTICLE INFO

Keywords:
InVEST
Climate change

ABSTRACT

An increasing number of people in the world are living in coastal areas characterized by high geophysical and biophysical sensitivity. Thus, it is necessary to provide coastal planners with tools helping them to design efficient management plans to mitigate the negative effects caused by a growing number of coastal climate

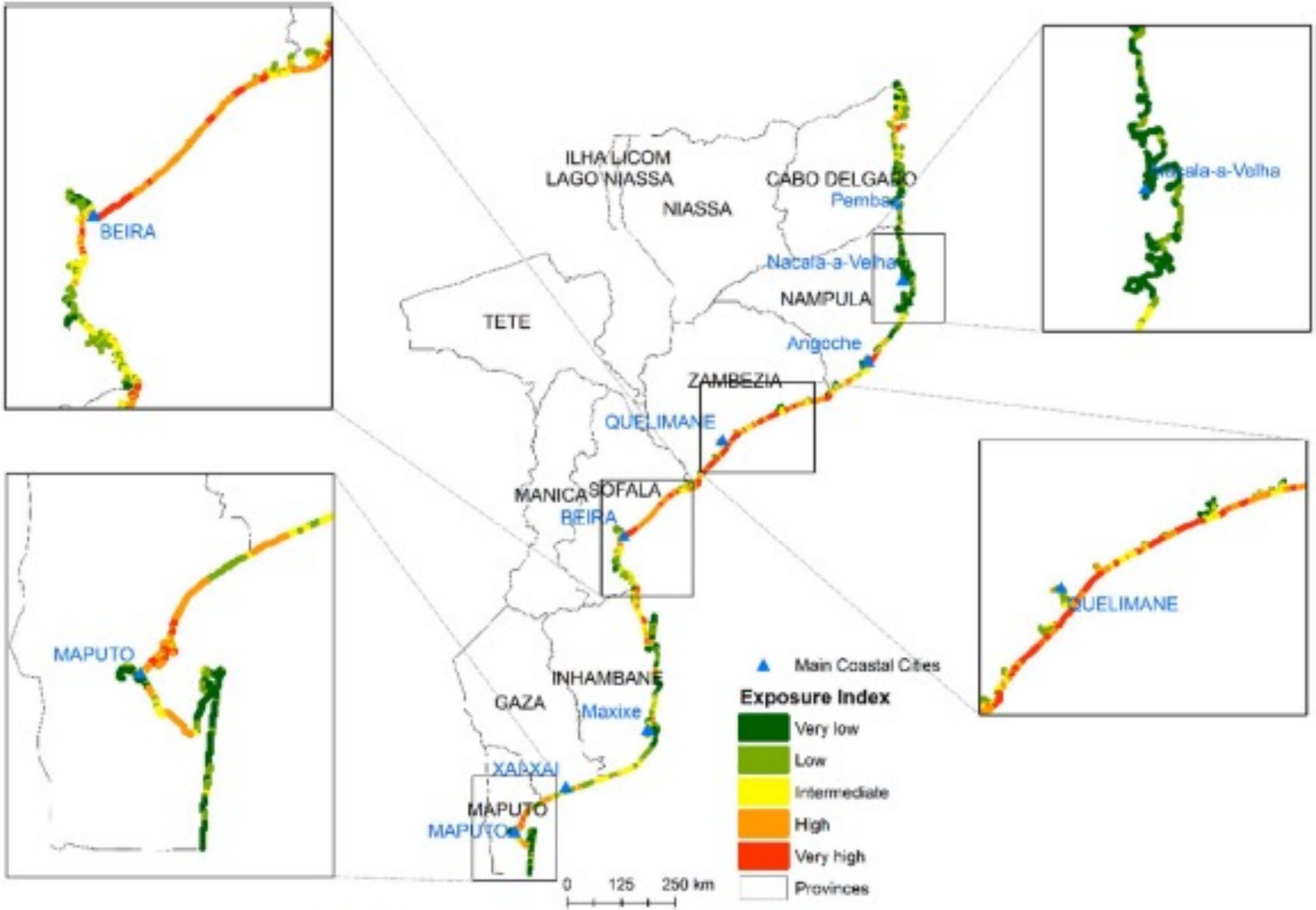

Fig. 2. Exposure Index for Mozambique in the "With habitats" scenario.

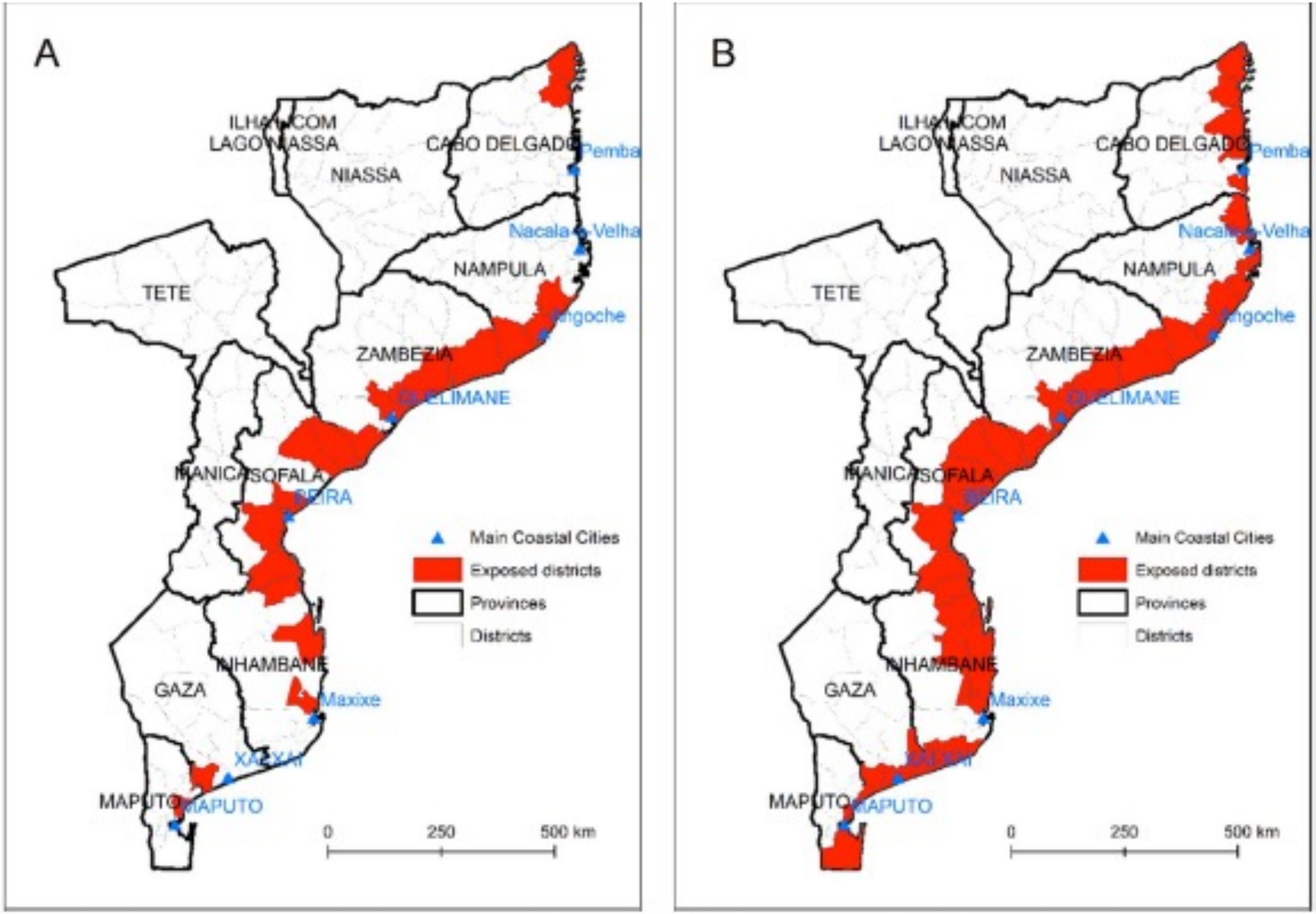

Fig. 3. Exposed districts in the "With habitats" (A, map on the left) and in the "Without habitats" (B, map on the right) scenarios.

Coastal Engineering 128 (2017) 106–122

Contents lists available at ScienceDirect

Coastal Engineering

journal homepage: www.elsevier.com/locate/coastaleng

Managing coastal erosion under climate change at the regional scale

Alexandra Toimil [*], Inigo J. Losada, Paula Camus, Pedro Díaz-Simal

Environmental Hydraulics Institute "IHCantabria", Universidad de Cantabria, Isabel Torres 15, 39005 Santander, Spain

ARTICLE INFO

Keywords:
Coastal erosion
Climate change
Regional scale
Probabilistic estimates

ABSTRACT

This study presents a comprehensive methodology that addresses climate change–induced coastal erosion at the regional scale O (100 km). The use of climate data with high space-time resolution enabled the reconstruction of the shoreline response to cross-shore forcing both historically and throughout the twenty-first century. Cross section–based equilibrium models were combined to assess beach erosion induced by local waves, storm surge,

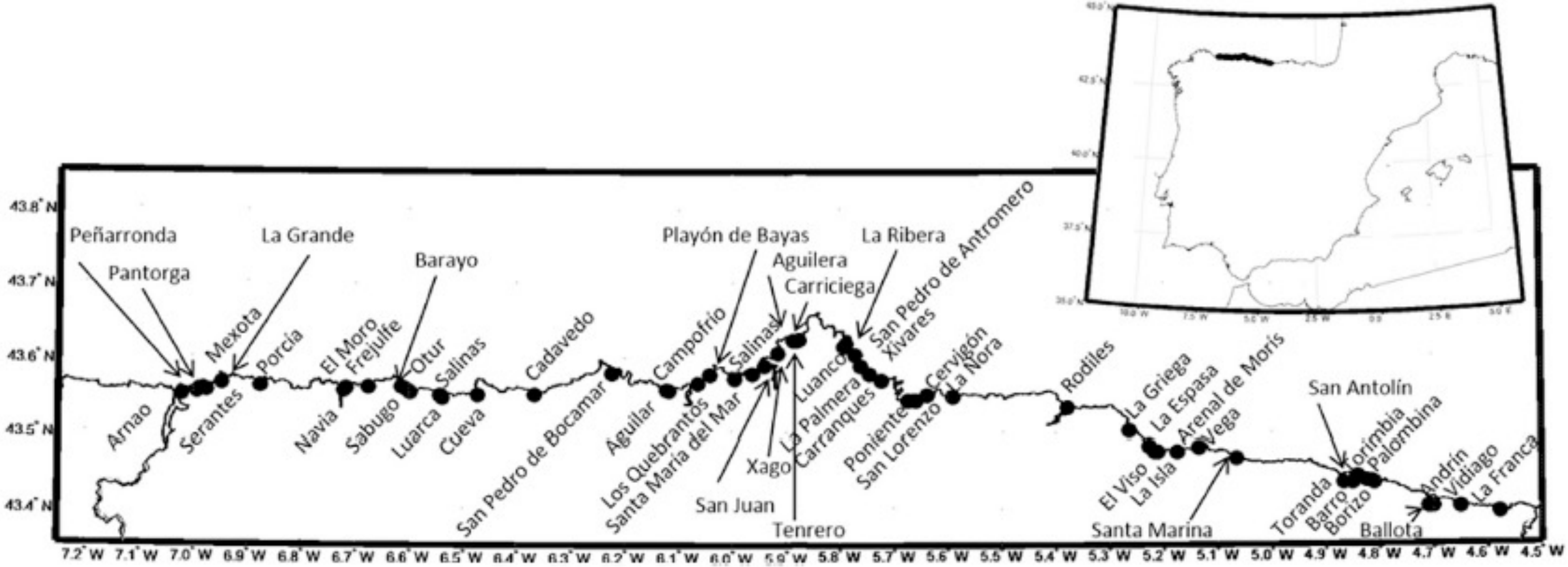

Fig. 1. Location of the Asturian beaches under study.

Changes in annual mean and extreme statistical wave and storm surge parameters under RCP8.5 for the period 2071-2099 with respect to 1979-2010

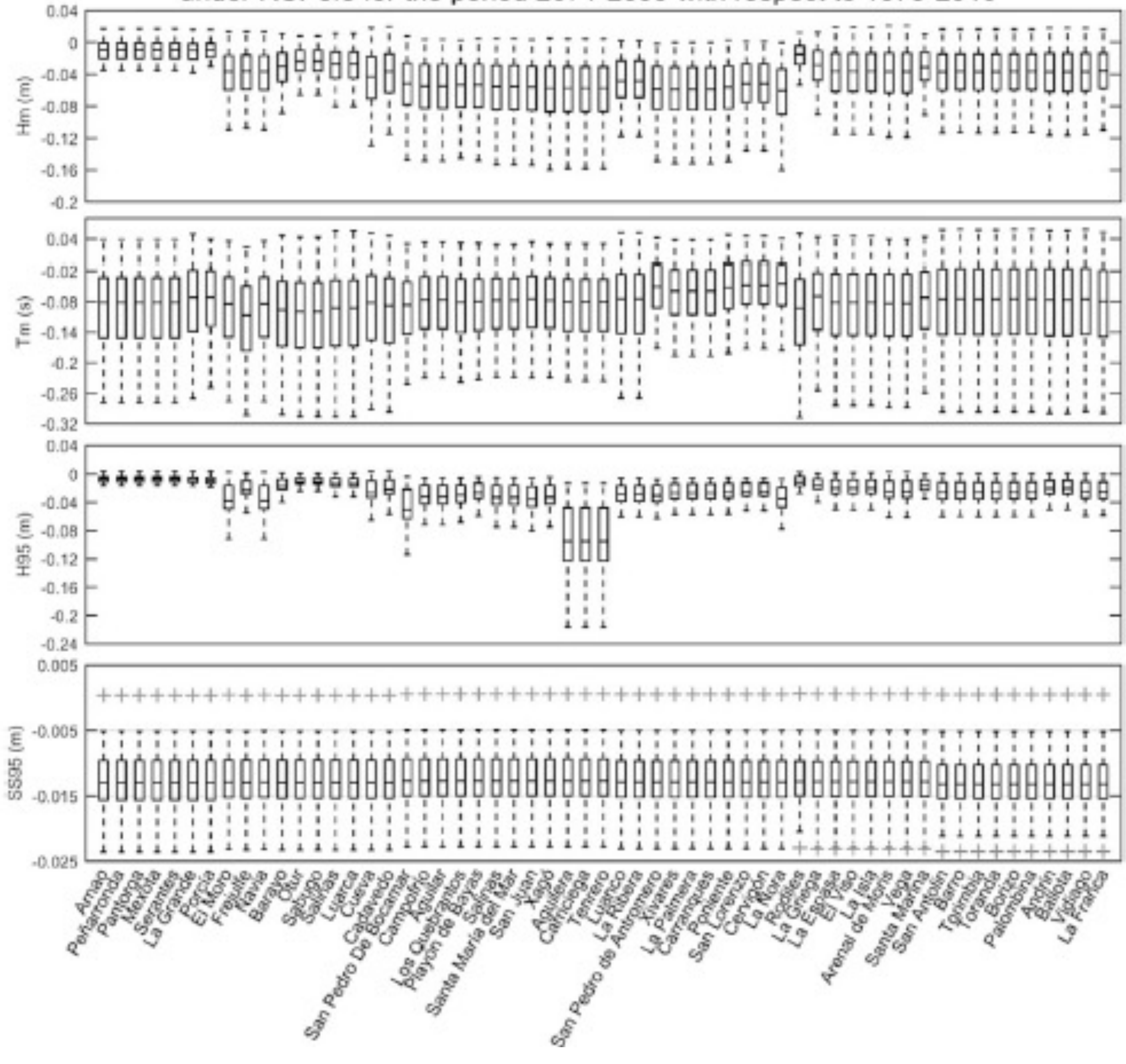

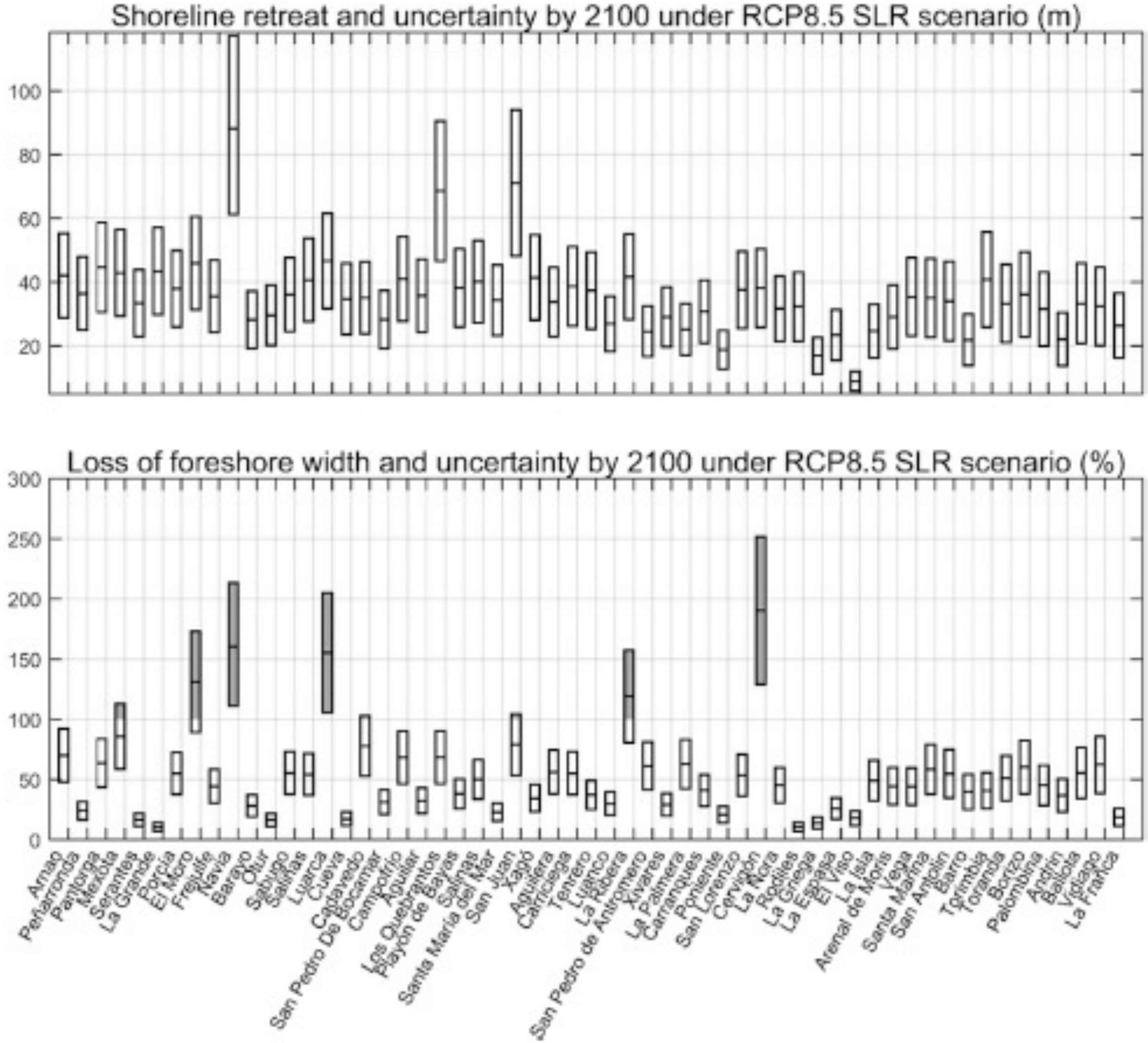

Shoreline retreat and uncertainty by 2100 under RCP8.5 SLR scenario (m)
100
80
60
40
20
Loss of foreshore width and uncertainty by 2100 under RCP8.5 SLR scenario (%)
300
250
200
150
100
50
0
Arnao
Peñarronda
Pantorga
Mexota
Serantes
La Grande
Porcía
El Moro
Frejulfe
Navia
Barayo
Otur
Sabugo
Salinas
Luarca
Cueva
Cadavedo
San Pedro De Bocamar
Campofrío
Aguilar
Los Quebrantos
Playón de Bayas
Salinas
Santa María del Mar
San Juan
Xagó
Aguilera
Carniciega
Tenrero
Luanco
La Ribera
San Pedro de Antromero
Xivares
La Palmera
Carranques
Poniente
San Lorenzo
Cervigón
La Ñora
Rodiles
La Griega
La Espasa
El Viso
La Isla
Arenal de Morís
Vega
Santa Marina
San Antolín
Barro
Torimbia
Toranda
Borizo
Palombina
Andrín
Ballota
Vidiago
La Franca

Ocean & Coastal Management xxx (2017) 1–15

Contents lists available at ScienceDirect

Ocean & Coastal Management

journal homepage: www.elsevier.com/locate/ocecoaman

Coastal erosion in central Chile: A new hazard?

Carolina Martínez [a, f, *], Manuel Contreras-López [b], Patricio Winckler [c], Héctor Hidalgo [d], Eduardo Godoy [d], Roberto Agredano [e, f]

[a] Instituto de Geografía, Pontificia Universidad Católica de Chile, Avda. Vicuña Mackenna 4860, Macul, Santiago, Chile
[b] Facultad de Ingeniería y Centro de Estudios Avanzados, Universidad de Playa Ancha, Chile
[c] Escuela de Ingeniería Civil Oceánica, Universidad de Valparaíso, Chile
[d] INGMAT R&D Center, José Miguel de la Barra 412, 4to piso, Santiago, Chile
[e] Departamento de Ingeniería Hidráulica y Ambiental, Pontificia Universidad Católica de Chile, Santiago, Chile
[f] Centro Nacional de Investigación para la Gestión Integrada de Desastres Naturales- CIGIDEN, FONDAP 15110017, Chile

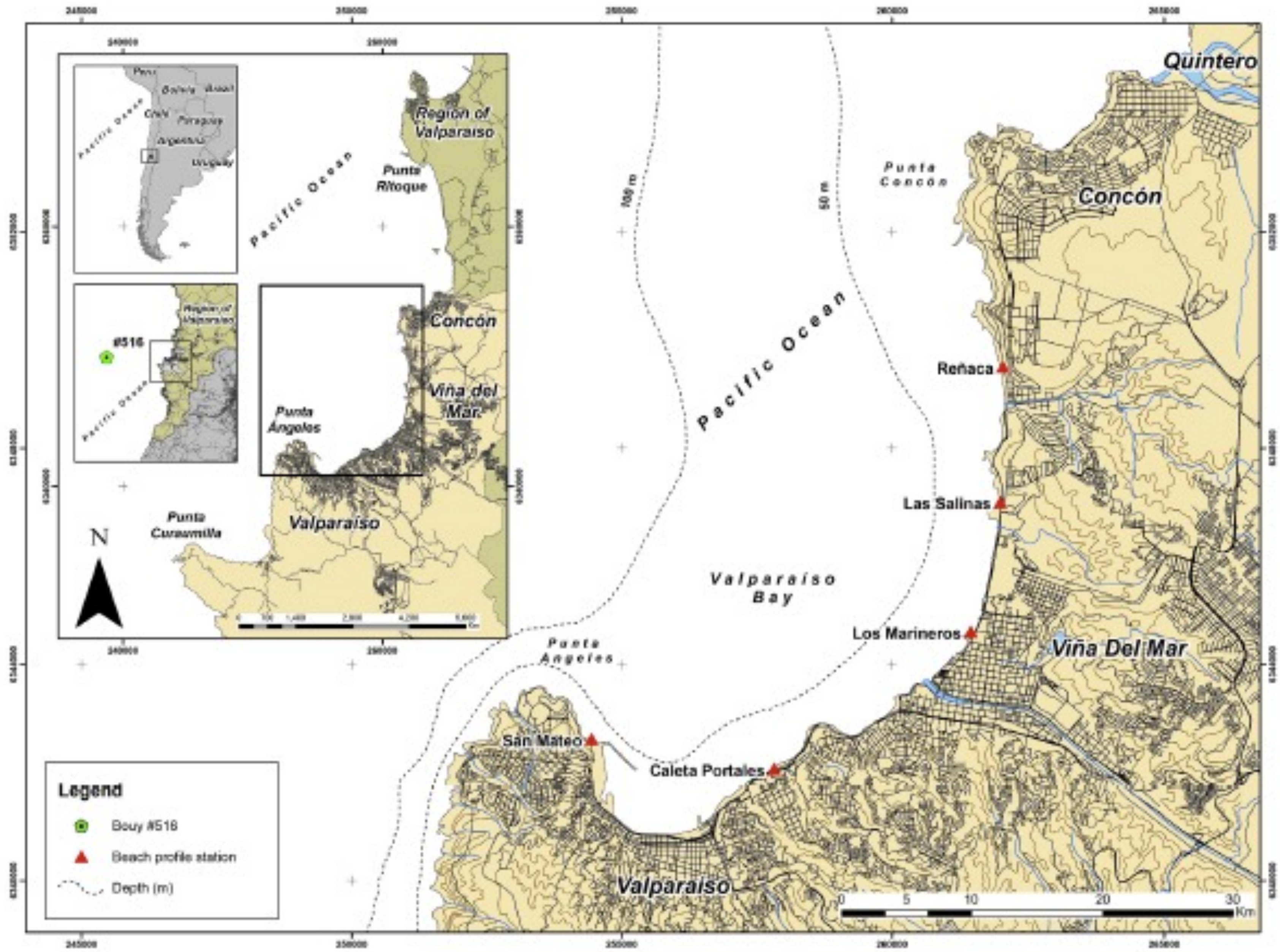

Fig. 1. Geographic context of the study area. The coast of Valparaíso-Viña del Mar forms part of the main metropolitan area of the country. The three main metropolitan areas of the country are coastal.

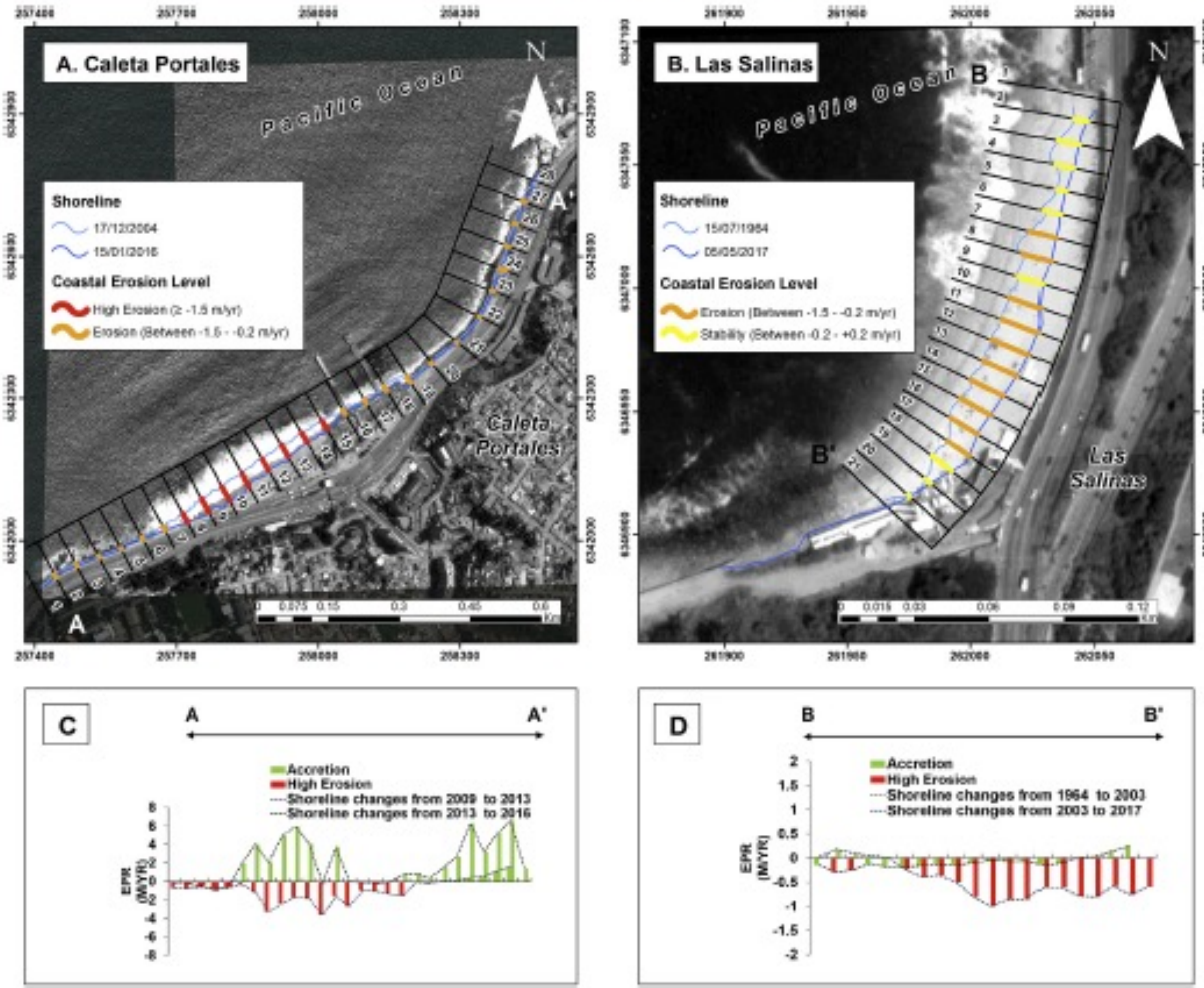

Fig. 3. Shoreline planform changes, Portales (a) and Las Salinas (b) beaches. These pocket beaches show the highest erosion rates, which is observed in their planforms. Figures B and C were made considering the criteria of Rangel-Buitrago et al. (2015).

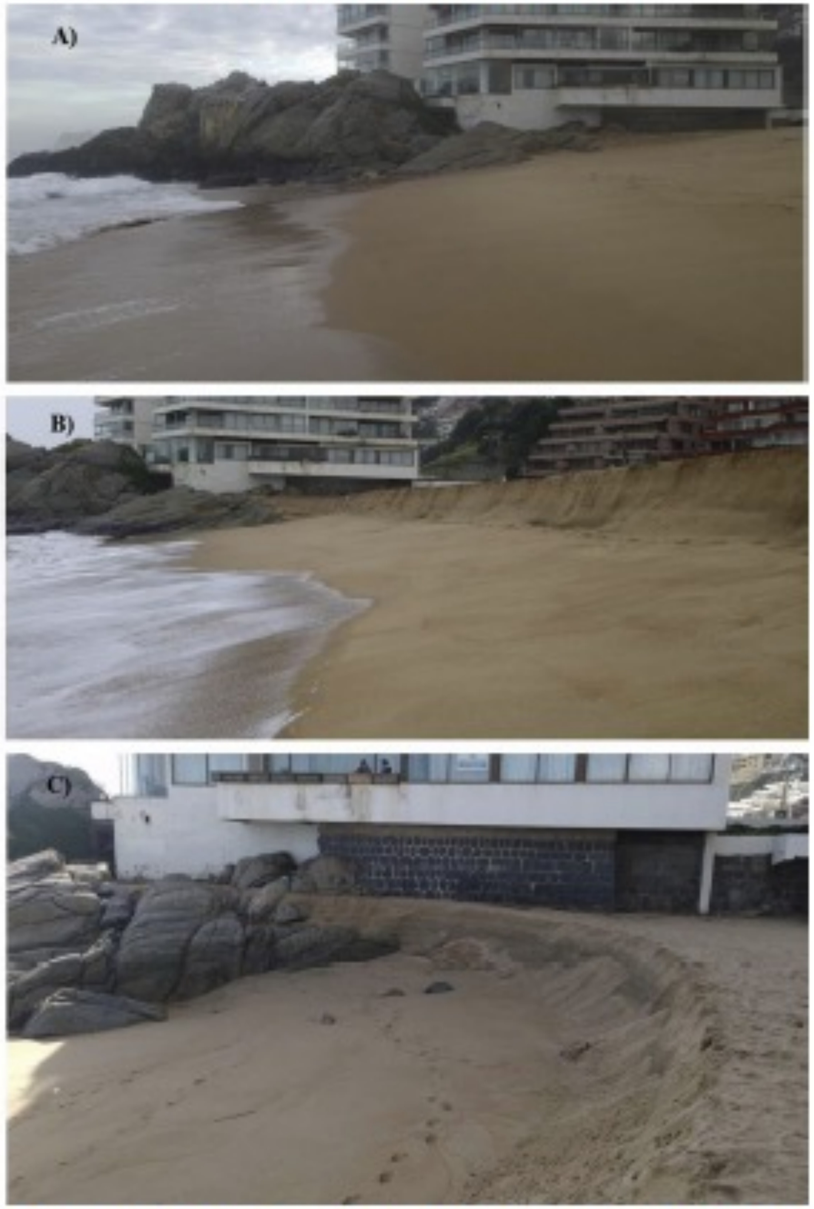

pe in the northern part of Reñaca Beach. The images were taken on (A) August 4th 2015, (B) August 7th and (C) August 10th; the dates among which storm events
e evolution of the vertical cut and the shoreline retreat are can be observed.

Table 2
Relative, average and total shoreline rate on urban beaches of Valparaíso and Viña del Mar. The time period considered in the erosion rate calculation is indicated in parentheses.

	Relative shoreline change (m/yr)										Average change (m/yr)			Total change (m)	
Beach	**Jul 1970**	**Jul 1986**	**Jul 2003**	**Dec 2004**	**Apr 2009**	**Jan 2013**	**Jan 2016**	**Sep 2016**	**Nov 2016**	**May 2017**	**Mean**	**Max**	**Min**	**Change**	**Erosion level**
Reñaca (1964-2016)	0.06			0.67	0.23	0.29			-0.02		0.24	0.67	-0.02	12.6	Accretion
Los Marineros (1964-2016)				0.31	0.05	-0.19	-0.18		-0.14		-0.03	0.31	-0.19	-1.6	Stability
Las Salinas (1964-2017)		0.41	-0.09		-0.10	-0.16	-0.26			-0.19	-0.06	0.41	-0.26	-3.3	Stability
Caleta Portales (1964-2016)					-0.76	-0.91	-1.19	-1.33			-1.04	-0.76	-133	-12.6	Erosion

Ocean & Coastal Management xxx (2017) 1–18

Contents lists available at ScienceDirect

Ocean & Coastal Management

journal homepage: www.elsevier.com/locate/ocecoaman

Hard protection structures as a principal coastal erosion management strategy along the Caribbean coast of Colombia. A chronicle of pitfalls

Nelson Rangel-Buitrago [a,*], Allan Williams [b,c], Giorgio Anfuso [d]

[a] Departamentos de Física - Biologia, Facultad de Ciencias Básicas, Universidad del Atlántico, Km 7 Antigua vía Puerto Colombia, Barranquilla, Atlántico, Colombia

[b] Faculty of Architecture, Computing, and Engineering, University of Wales: Trinity Saint David (Swansea), SA1 6ED, Mount Pleasant, Swansea, Wales, United Kingdom

[c] Interdisciplinary Centre of Social Sciences, (CICS.NOVA.FCSH/UNL), Avenida de Berna, 26 C, 1069-061, Lisboa, Portugal

[d] Departamento de Ciencias de la Tierra, Facultad de Ciencias del Mar y Ambientales, Universidad de Cádiz, Polígono río San Pedro s/n, 11510, Puerto Real, Cádiz, Spain

Table 3
Current coastal protection structures present along the study area (1: Absent, 2: Experiment, 3: Infrequent, 4: Moderately present, 5: Frequent).

STRUCTURE		DEPARTAMENT							
		GUAJIRA	MAGDALENA	ATLANTICO	BOLIVAR	SUCRE	CORDOBA	ANTIOQUIA	SAN ANDRES
Seawall	Concrete	4	4	4	5	5	4	4	4
	Bricks	2	2	2	2	2	2	2	2
	Stones	4	4	4	4	4	4	4	4
	Wood	1	1	1	1	1	1	1	1
	Fibreglass	1	1	1	1	1	1	1	1
	Gabions	1	2	2	2	2	1	1	1
Revetment (interlocking blocks)	Natural Stones	3	3	3	3	3	3	3	3
	Concrete s/bags	3	3	3	3	3	3	3	3
	Gabions	1	1	1	1	1	1	1	1
Rubble mound or Rip-Rap		4	4	4	4	4	4	3	3
Surfing reefs		4	1	1	1	4	1	1	4
Detached Breakwaters	Rocks	3	4	1	5	5	4	4	1
	Concrete	1	1	1	1	1	1	1	1
Groins	Emerged	5	5	5	5	5	5	5	5
	Submeged	5	5	5	5	5	5	5	5
	Mixed	5	5	5	5	5	5	5	5
	Permeable	2	1	2	3	3	3	2	2
Beach Nourishment	Sand	1	3	1	3	2	2	2	2
	Gravel	1	1	1	1	1	1	1	1
Dunes	Reconstruction	1	1	1	1	1	1	1	1
	Stabilization	2	1	2	1	1	1	1	1
	Construction	1	1	1	1	1	1	2	2
Posidonial and or mangroves	Natural	1	2	2	1	2	1	1	1
	Artifical	1	2	2	1	2	1	1	1
Cliff Stabilization		1	1	2	1	1	2	2	1
Tyres		3	3	2	2	1	2	2	2
Jetties		1	2	2	2	2	2	2	2


a)
b)
c)
d)
e)
f)
g)


a)
b)
c)
d)
e)
f)
g)


a)
b)
c)
d)
e)
f)

Km 18 - 21 (Road between Barranquilla - Santa Marta)

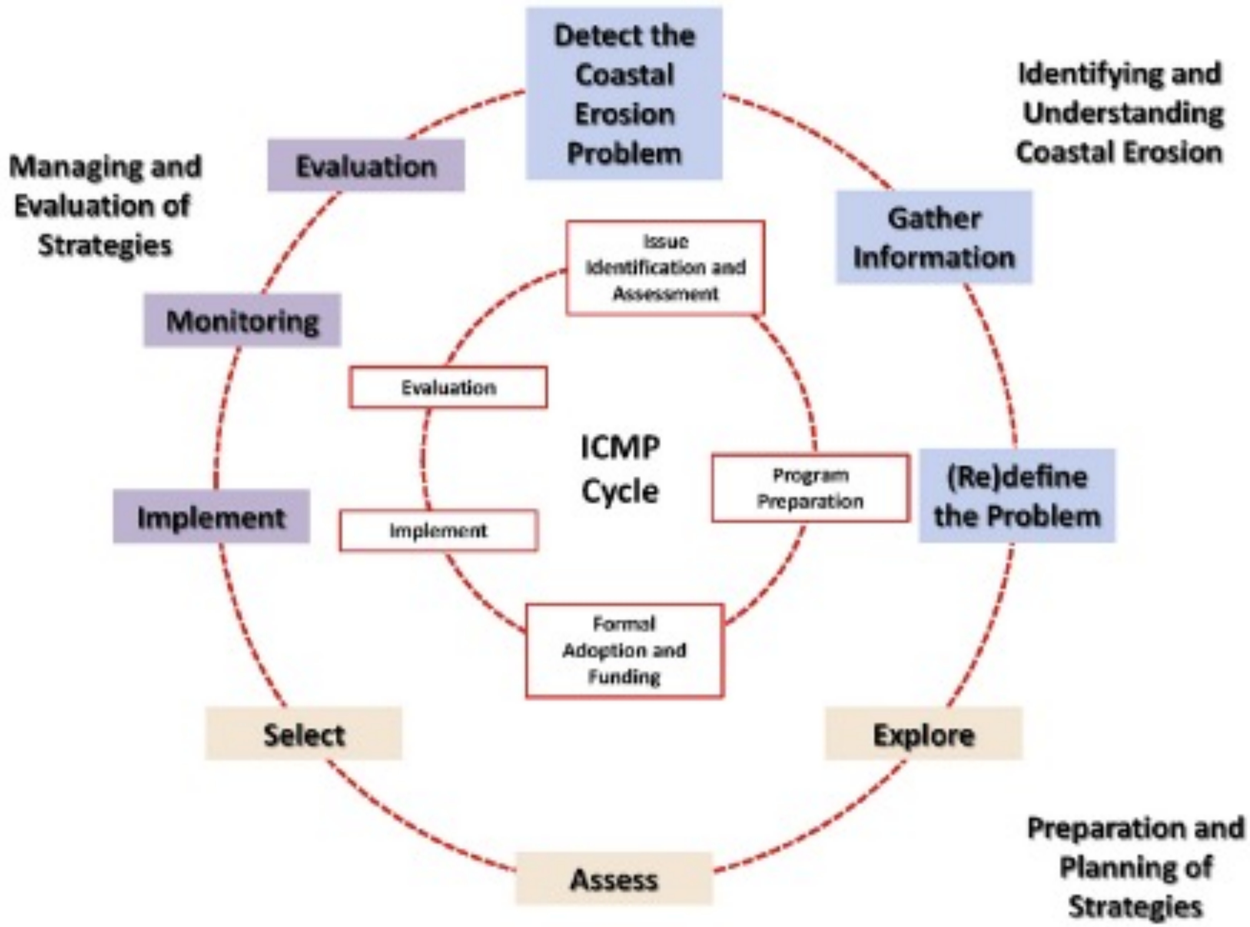

Detect the Coastal Erosion Problem
Identifying and Understanding Coastal Erosion
Managing and Evaluation of Strategies
Evaluation
Gather Information
Issue Identification and Assessment
Monitoring
Evaluation
ICMP Cycle
Program Preparation
(Re)define the Problem
Implement
Implement
Formal Adoption and Funding
Select
Explore
Assess
Preparation and Planning of Strategies

DEPARTMENT OF THE ARMY
U.S. Army Corps of Engineers
Washington, DC 20314-1000

EC 1110-2-292

CECW-EH

Circular
No. 1110-2-292

31 March 1998

Coastal Engineering Manual
Part III
Chapter 2
LONGSHORE SEDIMENT TRANSPORT

Table of Contents

Page